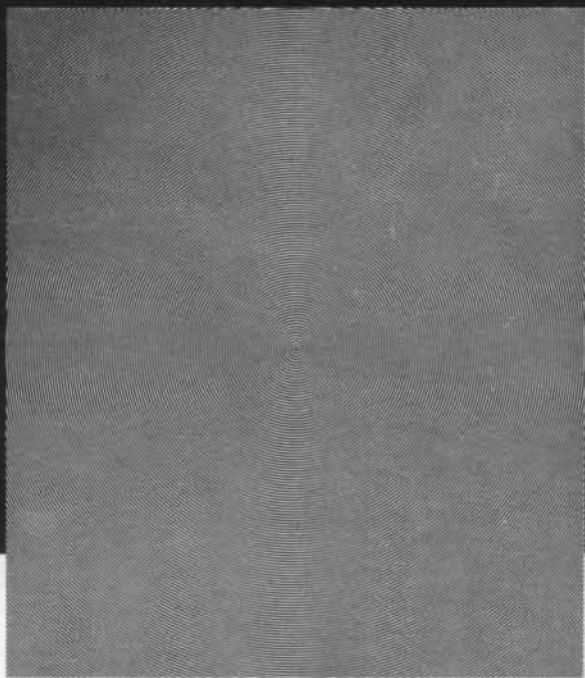
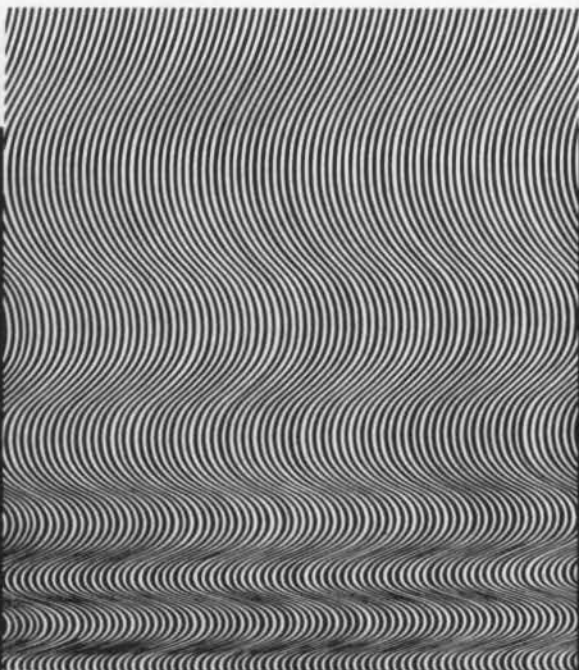


The Science of

MOIRÉ Patterns

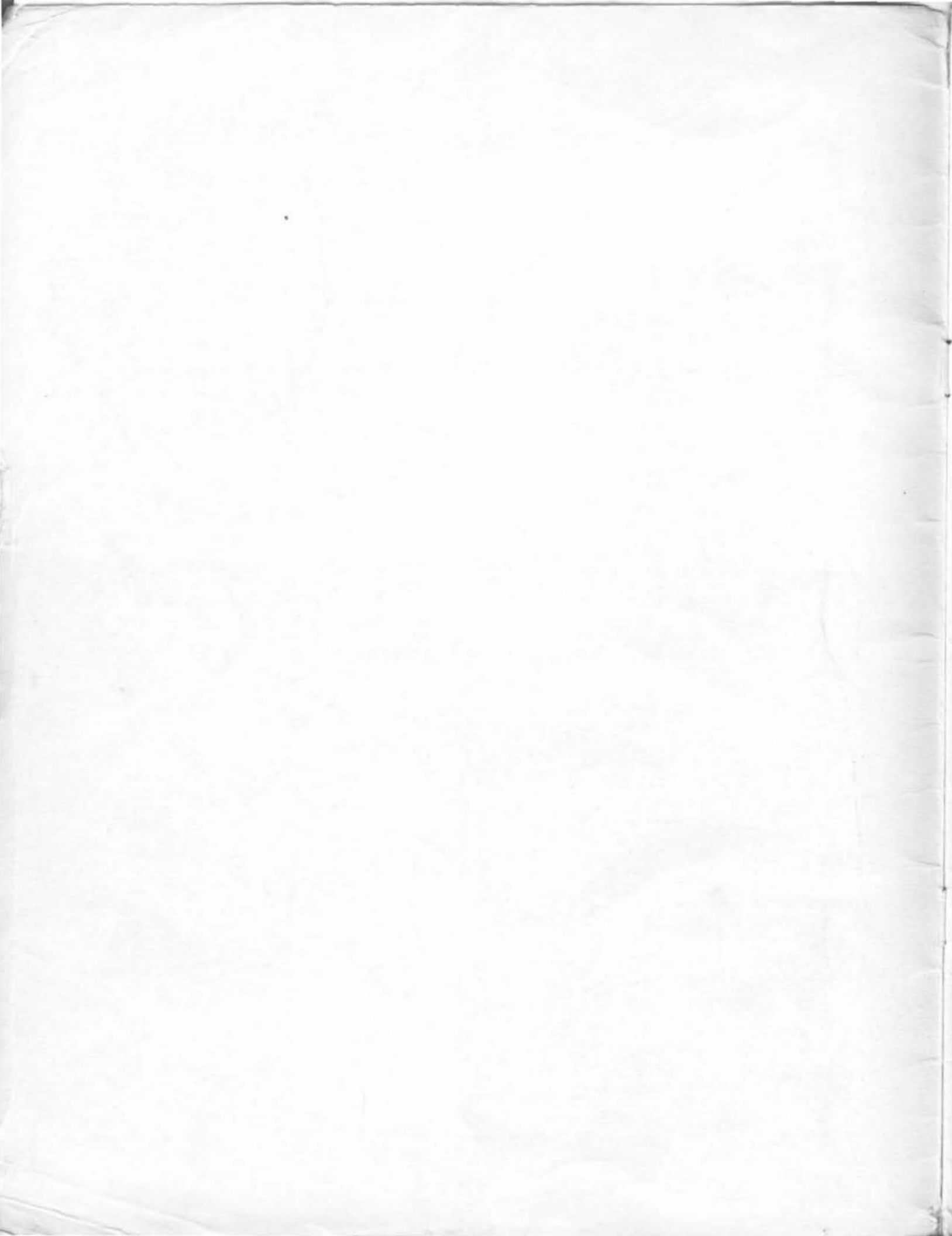


by Gerald Oster

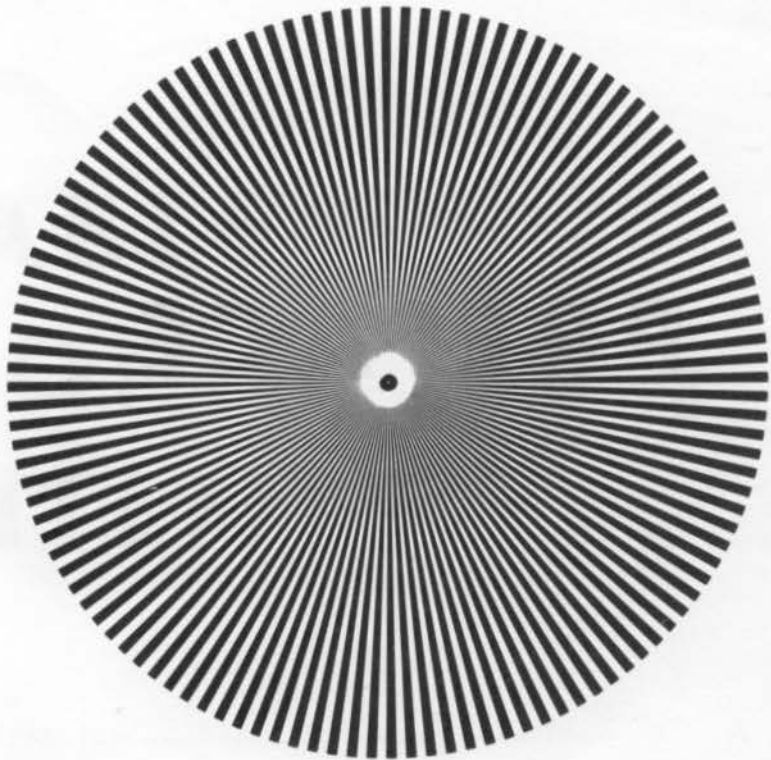


No. 9068 \$2.00 — Copyright 1964

EDMUND SCIENTIFIC CO., BARRINGTON, NEW JERSEY 08007

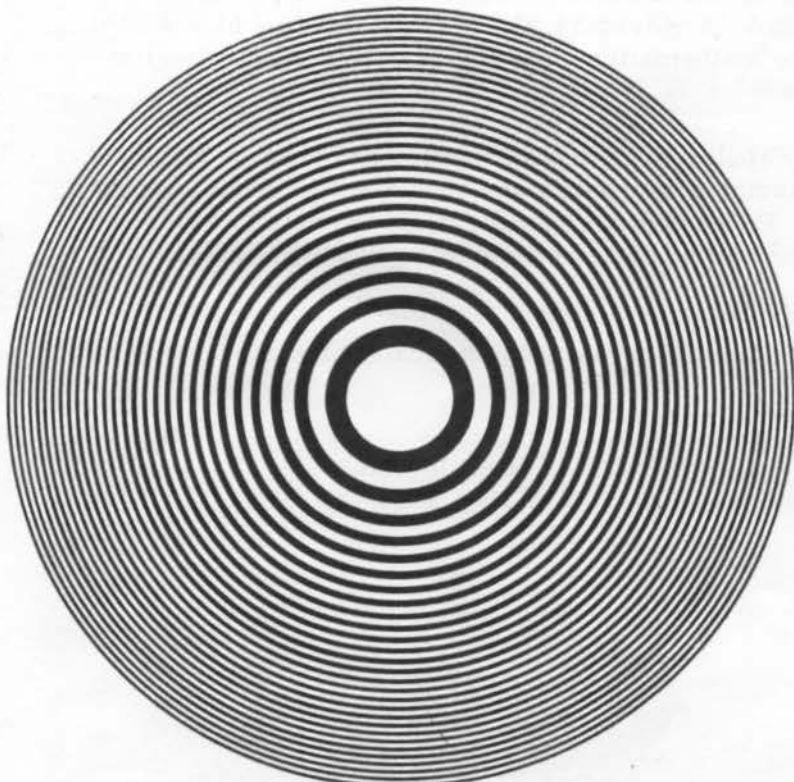


**PATTERN NO. 4 -
Radial Lines, 5°**



The original purchaser of this book receives an 8" x 10" woven fiberglass screen inserted at this page. It shows you the moirés produced by overlaying the square mesh pattern (20

squares per inch) over the Radial and Fresnel Patterns reproduced here. Keep this screen with the book, as it is used to demonstrate moiré phenomena in the following discussion.



**PATTERN NO. 6 -
Fresnel Zone Plate**

PREFACE

Polytechnic Institute of Brooklyn
Brooklyn, New York

This book is intended to give the reader some feeling for the exciting world of moiré patterns. To be really meaningful, the reader must actually perform the moiré experiments himself.

I have prepared for the Edmund Scientific Co. a moiré kit. No prior knowledge is necessary to enjoy working with the kit. In order to fully appreciate the power of the moiré technique, however, this book should be studied. To follow most of the arguments in the book (with the possible exception of parts of Sec. V and the Appendices) only a knowledge of high school mathematics is necessary. Conversely, an alert high school student may be inspired to study more mathematics since moiré patterns are visualizations of many concepts in mathematics.

The moiré technique has many applications to mathematics and physics including theoretical physics. Some of the examples treated in the book are concerned with my research problems now in progress. Psychologists, designers, and artists likewise can benefit from this book because the moiré technique reveals many of the peculiarities of human vision.

It is hoped that the reader will find moiré patterns aesthetically pleasing as well as intellectually stimulating.

Gerald Oster
May, 1964

TABLE OF CONTENTS

I.	Moiré Patterns in Everyday Life	Page 6
II.	The Moiré Kit.....	7
III.	Seeing Moiré with Screens.....	10
IV.	The Simplest Case-Parallel Equispaced Lines.....	11
V.	The General Approach to Moiré Patterns.....	13
VI.	Interpretation of Moiré Patterns in Terms of Projective Geometry....	16
VII.	Application of the Moiré Technique to Physics	18
VIII.	Visual Psychology of Moiré Effects	22
	Appendix A: Overlapping of Equispaced Gratings	25
	Appendix B: Focal Length Determination.....	26
	Appendix C: Theory of the Screen Determiner	27
	Appendix D: Overlapping on to a Variable Spaced Grating.....	28
	Appendix E: Experiments with Calcite Crystals.....	30
	References.....	31

I. MOIRÉ PATTERNS IN EVERYDAY LIFE

You have, no doubt, noticed the patterns produced by overlapping window insect screens or by the folds in a nylon curtain. Did you notice how the pattern changes wildly by slight movement of the screens? These patterns are called moiré (pronounced MW A R E H) patterns. The term moiré is from the French word for watered, as in watered or moiré silk. Such shimmering silk fabric was produced by the Chinese in ancient times.

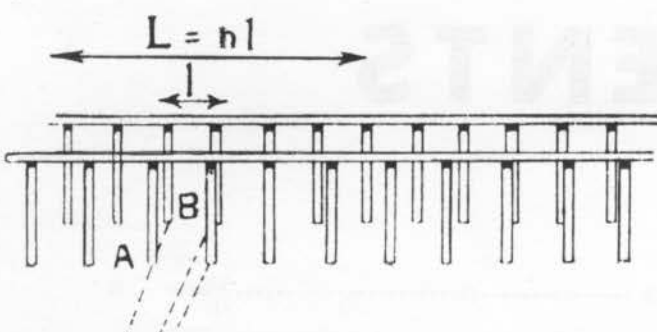


FIG. 1 Two parallel railings (A and B) produce a moiré (beat) pattern. The dotted lines point to the observer. The length L of the beat will contain n posts each separated by a distance l . (from M. Minnaert, "Light and Colour in the Open Air", G. Bell and Sons, London).

Moiré patterns are seen wherever a repetitive structure is overlaid with another structure and the line elements are nearly superposed. For example, two sets of railings on a bridge produce a moiré pattern (Fig. 1). The distance between the posts nearer us appears slightly greater than those further away and so we see a beat when a post of the nearer railing catches up with one of the further railing. The beat runs along faster than our actual movement. You can also see moiré patterns in wire trash cans. If you look at it in a certain direction you will see a huge enlargement of the repeat unit in the wire mesh. This is another feature of moiré, it magnifies repeated structures.

Look through a screen door at the landscape. (Note: this experiment works particularly well for nearsighted persons while not wearing glasses.) Wherever some structure in the landscape has elements of apparently the same repeat unit as the screen, a moiré pattern will appear in the door. Such repeat structures include shingles, bricks in a wall, or even windows

of a large apartment house. In other words, by the moiré technique we pick out periodic structures from an otherwise random landscape. Mathematicians would call this process a Fourier analysis.

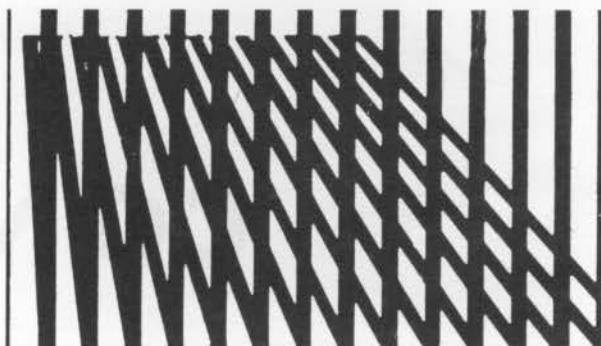


FIG. 2 Moiré pattern produced by a fence and its own shadow.

The moiré patterns produced by radiating lines can be very striking. For example, a picket fence when illuminated with the sun at an angle has a shadow which fans out. The moiré pattern produced by the fence and its shadow consists of curved lines (Fig. 2). If you observe at a distance of over 50 feet a forest behind the radiating lines of an old fashioned string hammock you will see a most magical effect especially as the hammock moves.

Despite the beauty of moiré patterns, some people try to avoid them. Imagine the chagrin of an architect who has designed a great structure but finds that the moiré patterns produced by the window screens with their reflection against the glass move madly about even with the slightest breeze and completely dominate the appearance of the building. Printers working with halftone screens in multicolor processes go to considerable pains to remove any moiré patterns (which appear as colored streaks) between the screens they lay down to produce the printed dots. All sorts of unwanted moiré patterns appear in television. Television entertainers are urged not to wear striped clothing. The slightest movement is transformed into a huge moving moiré pattern filling the entire TV screen. Along these lines, when you are at the zoo, look at a zebra some distance from the screen of his cage. You will see his breathing as an enormously enlarged moiré pattern.

Moiré patterns can be explained. Before trying to do so, let us first examine the moiré kit.

II. THE MOIRÉ KIT

The moiré kit consists of figures which have been constructed with great precision. We shall give a number to each of them so that we can conveniently refer to them. Each design is printed on clear film as a transparency, and also as an opaque positive of the transparency. For greatest precision, the printed side of the transparency should be in direct contact with the opaque print. The transparency and the opaque print are in correct contact when you can read, "Edmund Scientific Co." on both. For most purposes, however, this procedure is not important.

There are several ways of viewing the figures to see the moiré effects. It is often sufficient to lay the transparency over the print. Another procedure, if only the screens or the transparencies are involved, is to view the overlayed figure with a photographic viewer. To display the result to others in a classroom an overhead projector (a) is desirable. For producing moiré by the shadow method a good intense source (b) should be used. You can also produce moiré patterns by the reflection technique for which you will need a front surface mirror (c). This procedure is only applicable for the superposing of one figure on its image. You can produce moiré patterns by casting the image of one figure on another by using a one-way mirror (d). Considerable flexibility is achieved by using two opaque projectors (e) and superposing the images of the two on a projection screen.

-
- (a) For example, Edmund No. 70,514 (Overhead Projector Kit - \$15.00)
 - (b) For example, Edmund No. 70,602 (Hi Intensity Lamp - \$17.50)
 - (c) For example, Edmund No. 40,041
 - (d) For example, Edmund No. 70,326
 - (e) For example, Edmund No. 70,199
-

THE TRANSPARENCIES (& THEIR PRINTS)

No. 1. Coarse grating: Black and white lines of equal thickness and each equal to $3/44 = 0.0683"$. This screen is used mainly to illustrate the origin of moiré fringes but is too coarse for most measurement uses.

No. 2. 65-Line grating: there are 65 black lines per inch. Here again the black lines are equal to the white spacings. Finer gratings of this type (Ronchi rulings) are available (f).

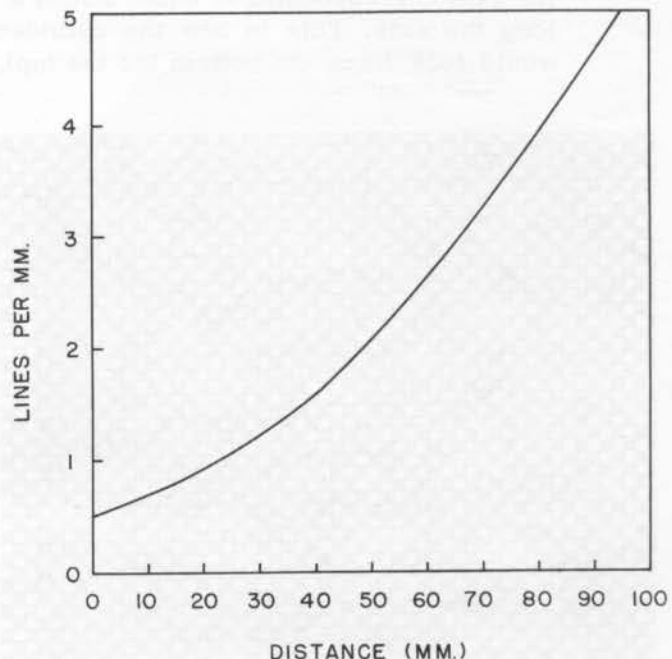


FIG. 3 Frequency of lines of No. 3 as a function of distance from the coarse end. The frequency is linear in line number (taking the coarsest line as line #1).

No. 3. Logarithmic spaced grating: Here the line frequency varies from 5 lines/mm. (127 lines/inch) on the fine line end to 0.5 lines /mm. (about 13 lines/inch) on the coarse end with spacing according to a logarithmic progression (see Fig. 3). For reference there are peaks every tenth line.

No. 4. Radial lines (5 degree): A circle is divided equally into 144 parts and the 72 alternate angles are blackened in, making 5 degree angular spacings.

No. 5. Equispaced circles: Equispaced concentric black circles, the frequency from the center is 65 lines per inch.

No. 6. Fresnel zone plate: These are concentric circles such that each blackened element and each white element is of equal area.

No. 7. Sphere projection: Imagine a sphere 3 cm. in diameter with rings painted on it corresponding to slices of equal thickness. This is how the sphere would look from the bottom (or from the top).

-
- (f) For example, Edmund No. 30,518 has 300 lines per inch, and No. 40,737 has 500 lines per inch.

No. 8. Cylinder projection: Imagine a cylinder 3 cm. in diameter with lines painted along its axis corresponding to equal slices along the axis. This is how the cylinder would look from the bottom (or the top).

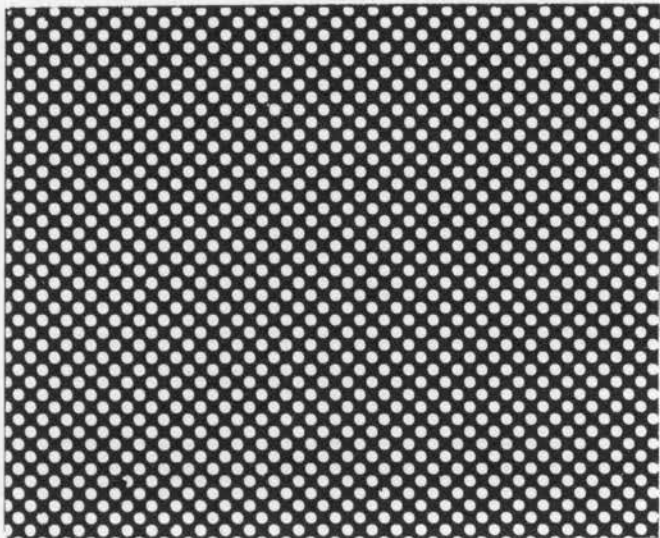


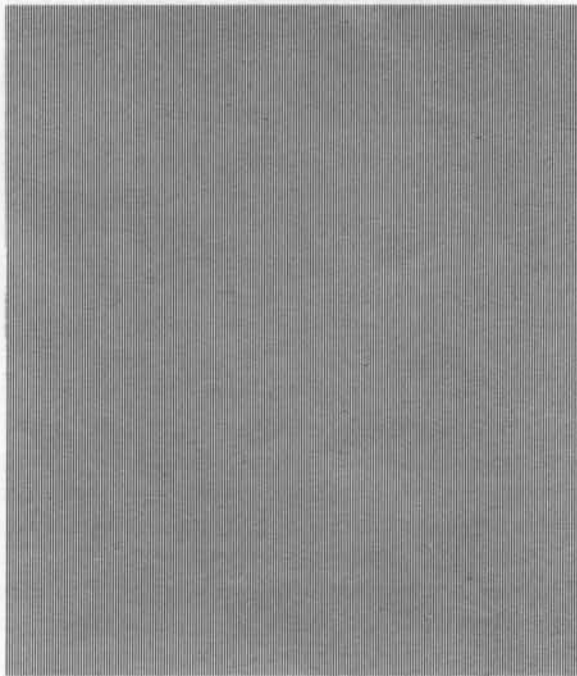
FIG. 4 Enlargement of the halftone screen (No. 9).

No. 9. Halftone screen (150): This consists of a square array of small circles, the repeat units being 150 to the inch. An enlargement of this screen is shown in Fig. 4.

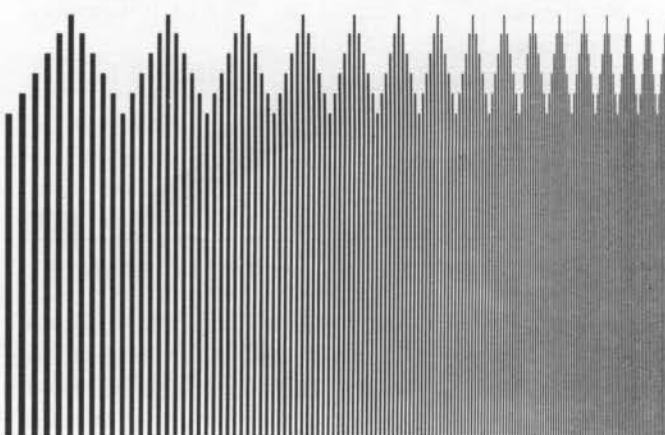
No. 10. Woven screen: The screen made of Fiberglass consists of square mesh with twenty squares to the inch. The screen 8 x 10" is inserted at the title page of this book.



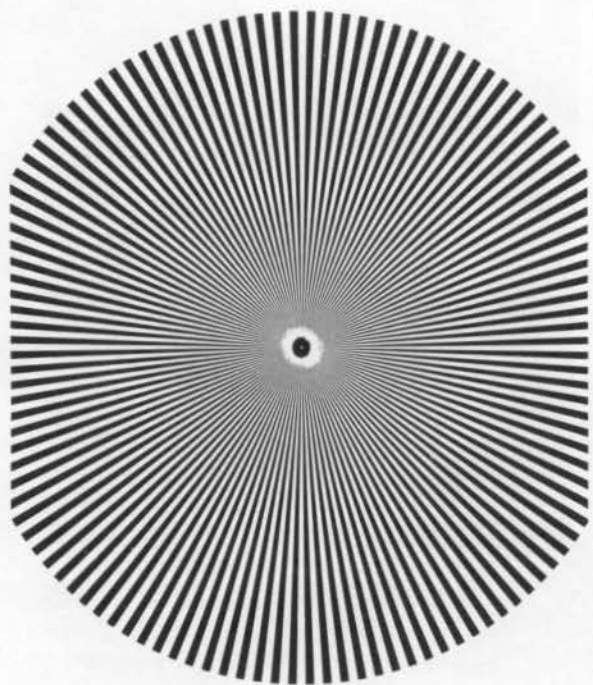
NO. 1



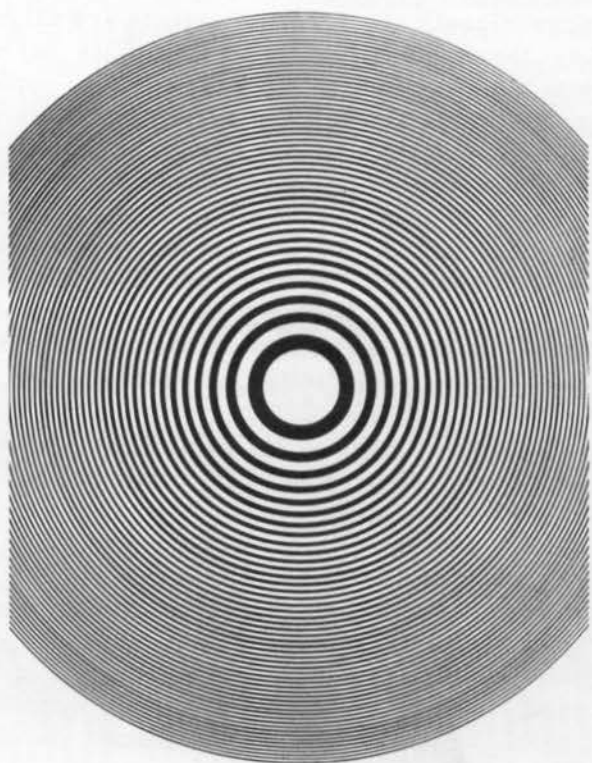
NO. 2



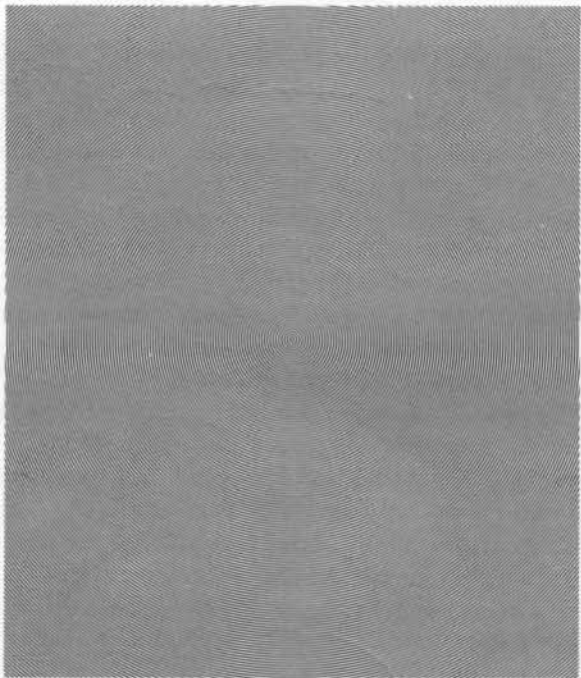
NO. 3



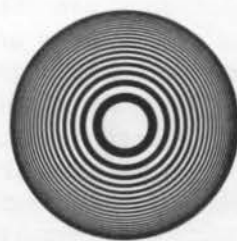
NO. 4



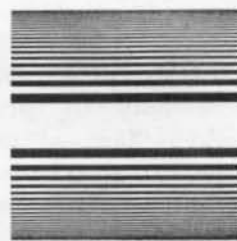
NO. 6



NO. 5



NO. 7



NO. 8

III. SEEING MOIRÉ WITH SCREENS

Hold the woven screen (No. 10) once folded at arm's length. Do you see the moiré patterns? Do you notice that the patterns become greater the more closely the screen elements are aligned? Lay the open screen on a flat white surface. Note the silky (moiré silky, to be sure) appearance. The shadow of the screen interacts with the actual screen to give the resultant pattern. Fold the screen loosely twice and then look through. Do you see the dots floating inside the three layers? A crystal may be regarded as a three dimensional screen. When X-rays are diffracted by a crystal, dots are produced. A crystal is a three-dimensional periodic structure whose periodicity is revealed by the X-rays.

Place one halftone dot screen (No. 9) on another and look through. Now rotate one slowly. Notice the dots grow in size. Starting from dots which cannot be seen by the naked eye they grow to tremendous size. This illustrates how by the moiré technique one can magnify periodic structures. A more striking case of moiré magnification is seen with diffraction gratings. An Edmund Scientific transmission-type diffraction grating (No. 40,267) when placed carefully and in perfect register over a reflecting-type diffraction grating (No. 50,201) with their ruled sides facing each other, produces a large saw-toothed moiré pattern. This represents a magnification of about 100,000 times! The evaluation of diffraction gratings by the moiré technique was first suggested by the British Physicist Lord Rayleigh in 1874 and has been developed in recent years at the National Physical Laboratory, England. (Ref. 1)*.

Another example of moiré magnification is given in electron microscopy (see Ref. 2). If a very thin crystal is placed over another thin crystal a moiré electron micrograph picture may be produced. This represents an enlargement of the basic repeat structure of the crystal lattice (Fig. 5). If the crystal has a defect, say a missing atom in a semiconductor, the nearby atoms shift from their normal lattice positions. The resultant moiré pattern due to the missing atom will show up in the electron micrograph. You can demonstrate the same sort of thing with the halftone dot screens. Make a slight crease in one the screens and align the screens so that the repeat unit is enlarged. The moiré pattern will be distorted in the neighborhood of the crease.

*References are given at the end of this book.

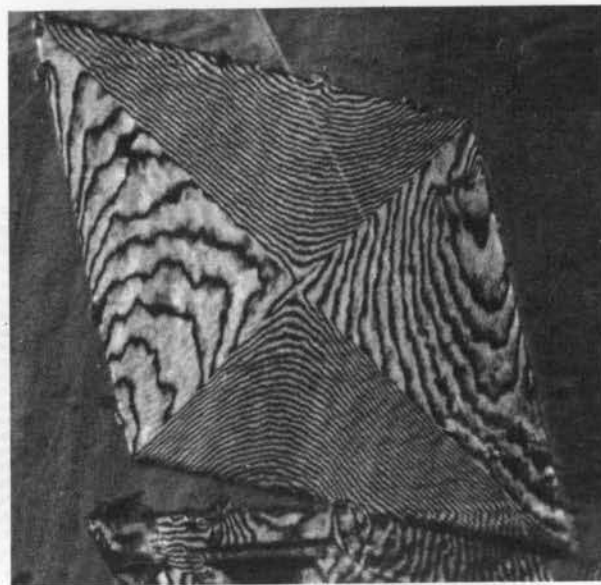


FIG. 5 Electron micrograph of polyethylene crystals. Two thin crystals placed one over the other in almost perfect register produces the moiré pattern. These crystals are pyramidal in form. (Courtesy of Dr. V. H. Holland, Chemstrand Research Center, Inc., Durham, N. C.).

The halftone dot screen is so called because it is used by printers to break up a continuous tone photograph (continuous tones ranging from white through grays to black) into dots to render it suitable for printing. If you place one screen over a printed picture and rotate the screen an enlarged dot pattern of the picture appears. Since our dot screen is very fine this effect is best seen with a high quality printed picture such as is on the cover of some magazines. Rotate the screen slowly and you will see enlarged sets of different colored dots as well as black dots. These are the different colored inks used in printing the picture. Art students can use this technique to advantage. If the screen is placed on illustrations in art books we can analyze the basic color components employed in the original painting assuming that the printed reproduction is of high fidelity.

The frequency of dots in a printed picture can be determined with an Edmund screen determiner (No. 40,751). This device consists of a family of fan lines which when placed over a periodic structure (half-tone screen, Ronchi rulings, etc.) produce rectangular hyperbolas. The

center of the family of hyperbolas determines the frequency of the periodic structure being examined. Along the edge of the determiner is a scale which gives directly the frequency in lines per inch. The theory of the device is given in Appendix C.

The dot pattern in photographs reproduced in newspapers is in the neighborhood of 60 lines per inch. Hence by laying the fine grating (No. 2) over such a picture, large spaced moiré lines will be produced at two orientations. Weaker and closer fringes are seen at intermediate angles. In

the same way one can examine the weave of some finely woven cloth, such as bed linen. Press No. 2 firmly against the cloth and moiré fringes will be seen at two orientations lying at right angles.

Thus we have demonstrated the moiré method as a microscope. Indeed a lensless microscope has been invented (by G. Oster and Y. Nishijima, see Ref. 3, page 59) which is based on the moiré technique. Similarly in Sec. I it was indicated how the moiré method can be employed as a telescope to enlarge periodic structures in a landscape.

IV. THE SIMPLEST CASE - PARALLEL EQUISPACED LINES

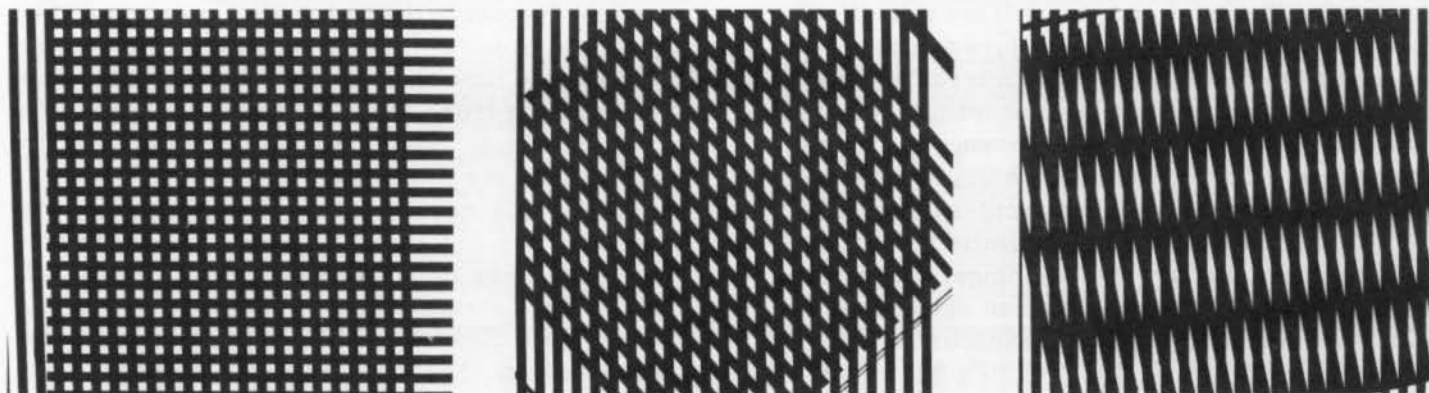


FIG. 6 Coarse gratings at A: 90°, B: 45°, C: some small angle.

The idea of the formation of a moiré pattern may best be illustrated with the coarse figure No. 1. Place No. 1 over its print with the lines perpendicular. One sees merely a square grid (Fig. 6A). Now rotate the top figure. When the lines make an angle of about 45° or less a new set of lines (the moiré fringes) appear (Fig. 6B). The moiré lines become more prominent as the angle is decreased. Also the distance between the fringes increases as the angle is decreased (Fig. 6C). The fringe distance appears to approach infinity when the angle approaches zero.

As shown in the Appendix A the distance between fringes is given by the equation

$$d = \frac{a}{2 \sin \theta/2} \quad (1)$$

where a is the repeat length of the figure and θ is the angle which the two figures make with one another. Thus for No. 1 $a = 0.0683"$ so that for $\theta = 45^\circ$ (the sine of 22.5° is 0.3827) the fringe spacing $d = 0.089"$. The equation shows that d is one inch when θ is about 4°. Since $\sin \theta$ approaches θ when θ is small we can express eq. 1 as

$$d \approx \frac{a}{\theta} \quad (2)$$

where θ (assumed small) is now in radians (one radian is about 57°).

From eq. 2 we see that the moiré technique offers a simple way of determining small angles. There is a limit to practical sensitivity because the fringes become less distinct as they become more separated. The fringes occur due to the space-filling differences. Where the lines cross there is least blackening so one sees white fringes. Adjacent on either side are the black lines (see also Sec. VIII).

Suppose the figures are not identical. Then the fringe spacing does not approach infinity as the angle between the lines becomes smaller. View the print of No. 1 through its transparency by holding the transparency a few inches above the print. The fringe distance becomes greater as we decrease θ but is finite even at zero angle. Since it is closer to our eyes, the apparent line spacing of the transparency is greater than that of the print. What we are observing at zero angle are beats. The black spacings of the transparency catch up and overtake the lines of the

print and fill in some of the white portions of the print in analogy to the fence posts in Sec. 1. As a consequence, one sees the beats at large intervals.

In Appendix A it is shown that the distance d between beats (the moiré fringe distance for $\theta = 0$) for two figures of spacing a and b , respectively, is given by

$$d = \frac{ab}{|b-a|} \quad (3)$$

where $|b-a|$ is the difference between the spacings. Thus the closer a is to b the greater will be the beat distance. Raise and lower the transparency above the print and you will see this effect. Hold the transparency No. 1 before a mirror. As you bring the figure close to the mirror the beats increase in distance and become infinite (that is, they disappear) when the transparency is pressed against the mirror. Interpose a glass plate between the transparency and a front-surface mirror. The moiré pattern will be finite. In fact, the moiré pattern is larger the thinner the interposing sheet. In this way we can determine the thickness (and uniformity) of transparent plastic films.

The simple expression Eq. 1 has a number of applications in the field of metrology (the science of measurement) described in detail in Ref. 4. For example, suppose $b = 0.0100$ cm. and $a = 0.0101$ cm., that is, a difference of 1 micron (about four ten-thousandths of an inch). Then we will see a beat of spacing of 1 cm. representing a magnification of 10,000 times. As an additional experiment, overlay a Ronchi grating of 150 per inch (Edmund No. 40,658) with one of 133 per inch (Edmund No. 40,656). Rotate one of them until the larger moiré pattern (that is, zero angle) is achieved. The beats will be $1/17$ inch apart in agreement with eq. 2 ($a = 1/133$ and $b = 1/150$ so $1/d = 150-133$). Incidentally, this is how one can make coarse gratings from fine gratings.

If you tilt the plane of transparency No. 1 when looking through it at a mirror you will see a beat pattern of the figure with its projected image. Here the beats are not uniformly spaced. A very small variation in angle of tilt will make a large displacement in the fringes. Conversely, if the figure is stationary and the mirror is tilted the same effect occurs. The combination of a grating and a mirror constitutes one of the most sensitive physical devices known. Indeed with the fine grating, No. 2, and a front-surface mirror it is possible to measure an angular difference to one part in a billion (see, for example, Ref. 5).

Here is an experiment to use the moiré technique for radio tuning. For this experiment you will need an oscilloscope and a radio (or audio) frequency oscillator. Tape the fine grating transparency No. 2 to the screen of an oscilloscope keeping the lines vertical. On the vertical plates of the oscilloscope impose a signal (works best with square wave pulses) and now vary the frequency. As the pattern of the signal approaches that of the transparency, moiré fringes (beats) will appear which get bigger and bigger as the frequency approaches that of the figure. Only at one precise frequency does the moiré pattern become infinite and is finite at either side of this frequency. This makes for fantastic sharpness of tuning. You will notice, however, that at the critical frequency the moiré pattern does not disappear at side edges of the signal images. This is because the time scale (the horizontal axis) of the oscilloscope trace is not linear at the edges. We shall return to this type of problem in another connection (see Appendix D).

Now let us consider the case where the line spacings are not equal and where the angle between the lines is not zero. Overlap the print of No. 1 with its transparency at an angle of roughly 10 degrees. Now maintaining this angle lift the transparency. Not only do the fringes become wider spaced but the moiré pattern rotates. You will notice that the fringes become more parallel to the lines of the print the higher the transparency is lifted.

As shown in Appendix A, the sine of the angle of which the moiré fringes make with original figure (the print) is given by

$$\sin \phi = \frac{b \sin \theta}{\sqrt{a^2 + b^2 - 2ab \cos \theta}} \quad (4)$$

The spacing of the fringes d is given by

$$d = \frac{ab}{\sqrt{a^2 + b^2 - 2ab \cos \theta}} \quad (5)$$

which becomes eq. 1 for $a = b$ and eq. 3 for $\theta = 0^\circ$.

In the experiment just described θ is about 10° and b is progressively increased as the transparency is lifted. For $a = b$ (the transparency in contact with print) then eq. 4 becomes (see Appendix A)

$$\sin \phi = \cos \theta / 2 \quad (6)$$

or, for our example $\theta = 85^\circ$. That is, the moiré fringes are nearly at right angles to the lines of the print. When the line spacing in the transparency becomes very large ($a \gg b$), say when

the figure is held about 6 inches or more above the print, $\sin \phi$ approaches zero, that is the moiré fringes become parallel with the lines of the print. Another feature of this phenomenon is that ϕ turns faster than θ . In fact, for small values of θ eq. 4 reduces to (note that for small x $\sin x \rightarrow x$ and $\cos x \rightarrow 1$)

$$\sin \phi \approx \frac{b \theta}{|a - b|} \quad (7)$$

That is, the smaller the difference in spacing the more sensitive is the dependence of the rotation of the moiré fringes on the value of θ .

Another way of changing the apparent spacings of a figure is to use a lens. An enlarging (convex) lens will, if held from the figure at a distance less than the focal length of the lens, increase the apparent spacings. Conversely a diverging (concave) lens will reduce the apparent spacings. Place a thin plano convex lens on the transparency of No. 2 and place these on the print of No. 2 so that large moiré fringes are seen. The moiré fringes in the lens area will be turned clockwise at an angle with respect to the background moiré fringes. A diverging lens will

turn the pattern in the opposite (counter clockwise) direction. The amount of turning is determined by the focal length of the lens and hence this constitutes a simple means of measuring the characteristics of a lens (or of a combination of lenses). The focal length f of the lens at a distance s from the transparency is given by

$$f = s \frac{\sin(\phi + \theta)}{\sin(\phi + \theta) - \sin \phi} \quad (8)$$

where ϕ is the angle turned from the background moiré fringes and θ is the angle of the two original figures. (Ref. 6. The derivation of eq. 8 is given in Appendix B.) For divergent lenses put in eq. 8 a minus sign before θ . In poorer lenses one sees curved moiré lines corresponding to a variation in focal length in the lens, that is, the lens has aberrations. A cylindrical lens when placed between gratings gives a helical ("barberpole") figure. Incidentally, lenses can also be studied by the moiré technique by placing the lens on top of two gratings which are separated by a small distance, rather than between the two gratings.

V. THE GENERAL APPROACH TO MOIRÉ PATTERNS

So far we have restricted ourselves to figures consisting of equispaced parallel lines. There is no reason why we should not consider variable spaced figures or, for that matter, radial lines or even curved lines such as concentric circles. As first pointed out by Oster and Nisijima (Ref. 3), moiré patterns should arise by the overlapping of figures containing any repetitive feature. We do require however, that the elements of the two figures be roughly the same size. Furthermore, the moiré pattern is most pronounced if the lines of one figure cross at a small angle with the lines of the other figure (see Sec. VIII).

We do not need to restrict ourselves to only two figures. We could overlap more than two figures to obtain still other moiré patterns. The nature of the resultant moiré pattern offers interesting problems in group theory which need not concern us here. It is important, however, to appreciate the endless varieties of patterns one can obtain. For the purposes of this book we shall be content to examine the elementary mathematics of the overlapping of only two figures.

There is a general method for calculating the moiré pattern expected for two given figures

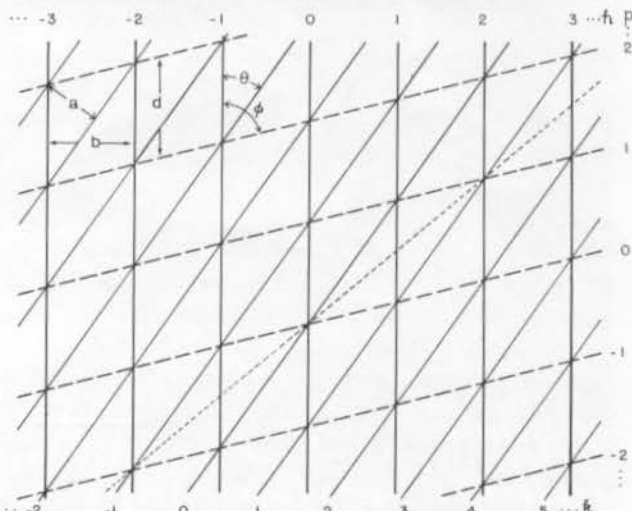


FIG. 7

Overlapping of grating of spacing a with grating of spacing b with the gratings inclined at an angle θ . Intersections indicated by dashed lines (the moiré fringes) satisfy the relation $h-k=p$ where p is the index for the moiré fringe. The moiré fringes are inclined with respect to the vertical axis (y-axis) by an angle ϕ and are separated by a distance d . The dotted line indicates a possible (but not vis-

ible) moiré fringe satisfying the relation $h - 2k = p$. Still other points of intersection can be connected such as those satisfying $h + k = p$ but such theoretically possible moiré fringes are not visible.

(see Ref. 6 for further details). Consider the case of two overlapping gratings of spacing a and b (see Fig. 7). We assign an integer $h = \dots -3, -2, -1, 0, 1, 2, 3, \dots$ to each vertical line and an integer $k = \dots -3, -2, -1, 0, 1, 2, 3, \dots$ to the other set of lines. A moiré pattern appears along the lines (dashed lines) of intersection of the elements of the figure. If the moiré fringes are assigned an integer $p = \dots -3, -2, -1, 0, 1, 2, 3, \dots$ then we note that the fringes connect points given by the equation (the indicial equation)

$$h - k = p \quad (9)$$

There are other points of intersection such as those along the dotted line where the indicial equation is given by $h - 2k = p$ but the moiré fringes are not perceptible. Still other points of intersection (running at a large angle with respect to the fringes) are given by $h + k = p$ but they too are not perceptible as moiré fringes since the lines of the figures cross at large angle. In other words, the dominant moiré fringes are those for which the lines of the figures cross at the smaller angle and at the same time the density of points of intersection are great. In Appendix A we consider the detailed geometry of the case of the overlapping of two gratings.

Now consider the case of the overlapping of a grating with a figure consisting of equispaced concentric circles. Place the transparency No. 5 on to the grating No. 2. You see two sets of parabolas. Now raise No. 5 and note the two sets of hyperbolas. Invert the positions of the two figures, that is, put No. 5 behind No. 2 and note the two sets of (incomplete) ellipses. If we call a the spacing between the concentric circles and b the spacings of the grating then we obtain parabolas, hyperbolas, and ellipses for $a=b$, $a>b$, and $a< b$, respectively.

The equation for a circle of radius r is given by $x^2 + y^2 = r^2$. Hence the equation for a circle of radius ha (h is an integer greater than zero) is

$$x^2 + y^2 = (ha)^2 \quad (10)$$

If we consider the lines of the grating as lying in the vertical (y axis) direction, then the equation for the line is

$$x = b k \quad (11)$$

where k is any integer (positive or negative). Solving for h in eq. 10 and for k in eq. 11 and inserting into the indicial equation, eq. 9, we obtain

$$(b^2 - a^2)x^2 \pm 2a bpx + b^2y^2 = a^2b^2p^2 \quad (12)$$

This is the general equation for a conic which describes parabolas, hyperbolas, and ellipses depending on the relative values of a and b . Any book on analytical geometry discusses eq. 11. We shall return to conics in Sec. VI.

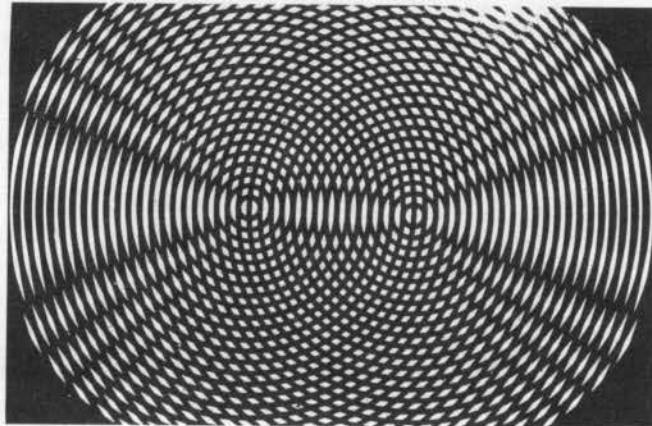


FIG. 8 Enlargement of the image produced by overlapping equispaced circles (No. 5) on to its copy.

Overlap the concentric circle figure No. 5 transparency on its print. Note the radiating lines. The number of radiating lines increases as the centers of the figures are drawn apart. You also will notice lens-like figures between the centers. Actually the radiating lines are the arms of hyperbolas whose foci are the centers of the two figures. Similarly the lens figures are ellipses with the two centers as foci. An enlargement of the resultant image is given in Fig. 8. The sets of hyperbolas and ellipses besides being confocal also constitute a set of orthogonal coordinates, that is, curves which cross at right angles. These are also called elliptic coordinates. The reader familiar with the theory of complex variables will recognize that they are the mapping on the z plane of $w = \sin z$ where z is the complex variable.

We can now prove the observed result by the indicial equation method. The equation for the circles of spacing a is

$$(x - s)^2 + y^2 = (ha)^2 \quad (13)$$

where s is the distance of the center of the figure from some point taken as the origin. Similarly for the other figure a distance s on the other side

of the point (that is, the center-to-center distance of the figures is $2s$) then the equation is

$$(x + s)^2 + y^2 = (ka)^2 \quad (14)$$

Eliminating h and k and inserting in the indicial equation, eq. 9, we obtain

$$\frac{x^2}{\left(\frac{ap}{2}\right)^2} - \frac{y^2}{s^2 - \left(\frac{ap}{2}\right)^2} = 1 \quad (15)$$

which is the equation of a hyperbola. The greater s is the greater the number of arms of the moiré pattern. Between the centers of the figures the indicial equation $h + k = p$ applies in which case we have a plus sign in eq. 15, that is, we have the equation of an ellipse.

There is a wide variety of other patterns which can readily be produced. For example, the transparency of the zone plate (No. 6) overlayed on its print produces equispaced parallel lines when their centers are close but when the centers are far apart a replica of the zone plate appears. These two cases correspond to the indicial equations $h - k = p$ and $h + k = p$, respectively. The equation for two zone plates separated from their centers by a distance $2s$ are given by

$$(x - s)^2 + y^2 = h/\pi \quad (16)$$

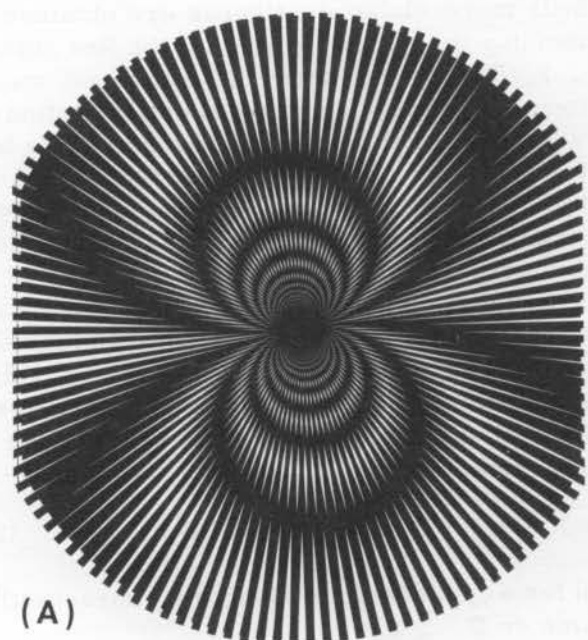
and

$$(x + s)^2 + y^2 = k/\pi \quad (17)$$

where each area of the black (or white portion) are equal and taken as unity. The parallel line moiré pattern has a spacing inversely proportional to the center-to-center distance of the two zone plates (Ref. 6).

When the woven screen (No. 10) is placed over the zone plate the whole field is filled with the zone plate figures, the most prominent of which lie along the directions of the fibers in the mesh. These correspond to the superposition of two grids at right angles each of which obeys the indicial equation $h - rk = p$ where $r = -3, -2, -1, 0, 1, 2, 3 \dots$

Place the radial lines figure (No. 4) over its print. When the centers are close one obtains a series of coaxial circles (Fig. 9A) with each circle passing through the center of the figures. When the centers are far apart one observes a series of rectangular hyperbolas (Fig. 9B). These moiré patterns correspond to the indicial equations $h - k = p$ and $h + k = p$, respectively. The equations for the radial figures (separated by a distance $2s$) are given by



(A)

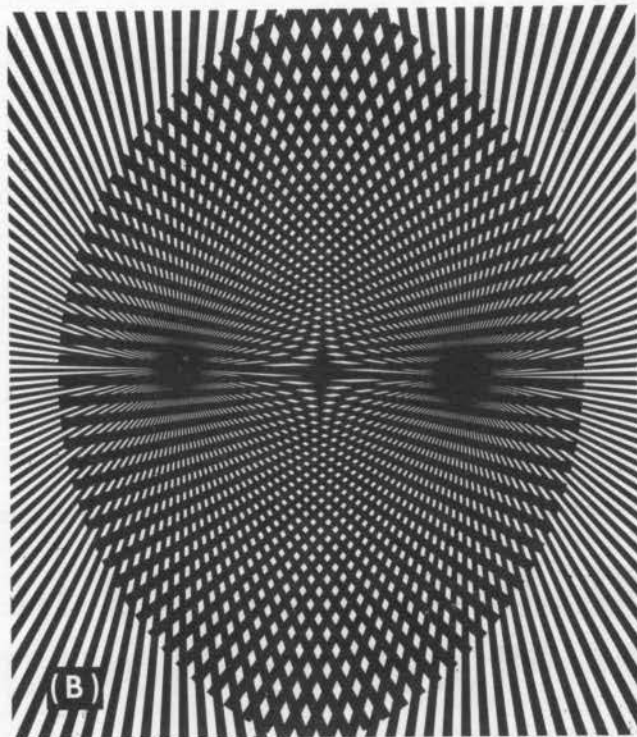


FIG. 9 Overlapping radial lines (No. 4) on to its copy with centers close (A) and far apart (B).

$$y = (x + s) \tan(k\pi/c) \quad (18)$$

and

$$y = (x - s) \tan(k\pi/c) \quad (19)$$

where c is the number of radiating lines of the figure.

Still more elaborate figures are obtained by combining the radial figure with the fine grating No. 2. There one sees the prominent moiré pattern corresponding to the indicial equation $h - k = p$ together with the weaker higher orders corresponding to $h - rk = p$ where r differs from unity. The woven screen placed over No. 4 gives a similar moiré pattern having a four-fold symmetry.

It is left to the reader to explore the moiré patterns produced with the sphere and the cylinder projections (No. 7 and 8, respectively). The equations for these two figures are for a sphere of diameter D where the slicings are of thickness a

$$x^2 + y^2 = ha(D-ha) \quad (20)$$

and for a cylinder (axis along the y direction) of diameter D

$$x^2 = ha(D-ha) \quad (21)$$

Note that for a sphere for which ah is much smaller than D the area of the circles (π times $x^2 + y^2$) is proportional to h just as for the Fresnel zone plate (the projection of a paraboloid).

The variable spaced grating (No. 3) is particularly convenient in that it contains a wide range of spacings. Thus it gives a moiré pattern consisting of parabolas (nearly) with weaker higher orders for line figures ranging from the fine grating (No. 2 gives a maximum at the tenth peak from the fine line end) to the woven screen. The spacing on No. 3 where the maximum in the parabola occurs tells the spacing of the grating being

examined. Combining No. 3 with the other figures gives results which are too involved to treat analytically but are of interest in other connections as seen in Sec. V and VI.

With a little ingenuity one can produce a great variety of patterns in other ways. For example, take the case analogous to the shadow of a fence mentioned in Sec. I. If the transparency of the coarse grating (No. 1) is placed with its plane at right angles to its print and with the stripes vertical, hyperbolas are seen through the transparency. The equation for the projection of the coarse grating (a fan) is

$$x = ha(1-y/c) \quad (22)$$

where c designates the distance to origin of the fan. This together with the equation for the print, namely $x = kb$, and the indicial equation, $h - k = p$, gives the resultant moiré pattern (Fig. 2). In Appendix C eq. 22 is explained further and applied to the case of the screen determiner.

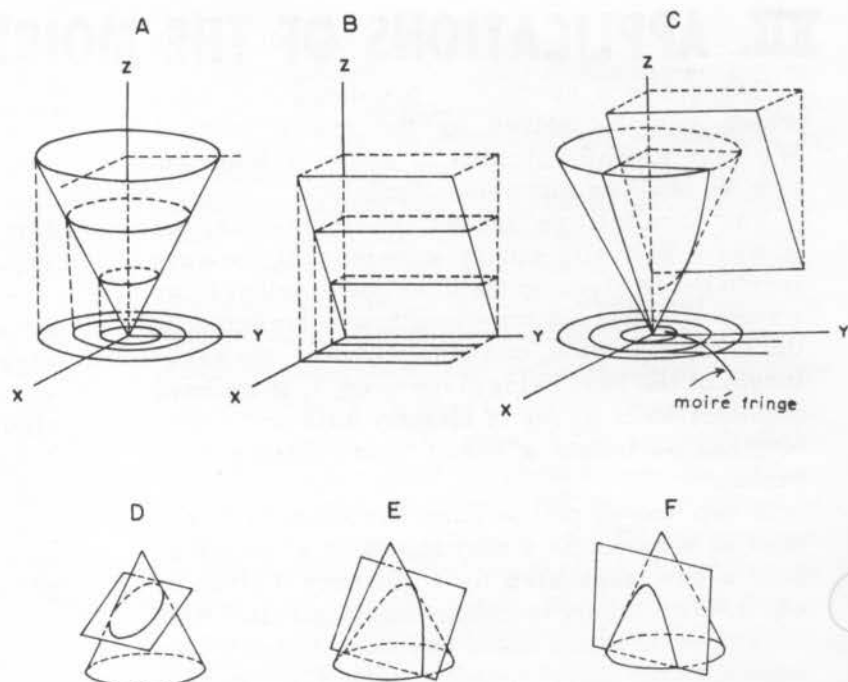
The concentric equispaced circles (No. 5) can be used to give complicated moiré patterns. When the transparency is held a few inches above its print and the centers do not coincide a moiré pattern consisting of a series of limacons-like is obtained (Ref. 7). The equation for the curves is of fourth order in x and y and can be derived from eq. 13 and from 14 (replace a by b). As a matter of fact, it is difficult to obtain anything but such curves. Only by very careful angular alignment can the centers of the two figures (held a few inches apart) be precisely placed one over the other, in which case, the moiré pattern abruptly reverts to a series of concentric circles of large spacing (the beat pattern).

VI. INTERPRETATION OF MOIRÉ PATTERNS IN TERMS OF PROJECTIVE GEOMETRY

There is another way of understanding moiré patterns, namely, in terms of projections. Take the case of the conics. Imagine that a cone had lines drawn on it at equal heights (see Fig. 10). Then its projection would simply be the equi-spaced concentric circle figure (No. 5). The closer the lines are, the more acute is the angle of the apex. A parallel line figure (either No. 1 or 2) could likewise be regarded as an inclined plane, the inclination being greater the smaller

the spacing. Now when we combine the cone projection, namely the concentric equispaced circles (No. 5), and the inclined plane, namely the parallel line figure No. 2, we are essentially producing conic sections. If the inclination of the plane is equal to that of the cone (that is, the interline spacings are the same) then we obtain parabolas. If the inclination of the plane is greater than that of the cone, one obtains hyperbolas. If the inclination is less we obtain ellipses.

FIG. 10 A. Projection of cone on x-y axis to give equispaced concentric circles, B. Projection of inclined plane on x-y axis to give grating, C. Intersection of cone with inclined plane to give moiré pattern on x-y plane, D. Conic section (ellipse) obtained by cutting cone with plane at small angle of inclination, E. Conic section (parabola) obtained by cutting cone with plane inclined parallel to the sloping edge of the cone, F. Conic section (hyperbola) obtained by cutting cone at high angle. (Figs. A, B and C are adapted from drawings by Mr. David W. Kammler who also drew the sphere and cylinder projections (No. 7 and 8, respectively).



As will be noticed, one obtains two families of curves, that is, two similar conic sections. This occurs because the direction of the inclination of the plane is not specified. It may come from one direction or from another.

In general we can say that since the equation for one set of figures defines a surface with intersections at $z=h$ and another defines a surface with intersections at $z=k$. Then by elimination (via the indicial equation) of h and k by superposition, we obtain the intersection of the surfaces projected on the x-y plane. Thus if we take the figure for spheres (No. 7) and the figure for cylinders (No. 8) their superposition gives a moiré pattern which is the projection of a cylinder intersecting a sphere. Perhaps a more readily appreciated intersection is that produced by a plane cutting a sphere. Take the variable spaced grating (No. 3) and apply it over the sphere (No. 7). As we move from the smaller spacing of No. 3 we see the sphere being cut first at a high angle at its edge and then progressively with a plane of lower inclination.

It is clear, therefore, that the moiré technique offers a convenient method of producing projections of any intersecting structures. One could also consider the intersections of more than two structures by overlapping three or more figures.

Because of the ambiguity of direction in the figures, in some cases one obtains two differ-

ent kinds of moiré patterns for the same figures. Take the case, for example, of the zone plates (No. 6) which is the projection of a paraboloid. When the centers of the two paraboloids are close, one observes moiré patterns consisting of parallel lines but when the centers are further drawn apart one observes rings between the centers. Here we are observing the projection of two interesting paraboloids. In the first case the paraboloids open in the same direction, but in the second, one is turned upwards and the second downwards. An analogous argument would apply to the case of the radial lines figure (No. 4) which is the projection of a helix (like looking down a winding staircase). Fig. 9A is like looking down the end of two helical screws turning in opposite directions while Fig. 9B is when the screws are turning in the same direction.

One can regard wood grain as being a moiré pattern. In the cross-section of a tree the annular rings approximate concentric equispaced circles (No. 5). When a plank is cut from the tree one obtains the intersections with the plane of the cut to give the grain. When the cut is parallel to the long axis of the tree (assumed a right angle circular cylinder) one obtains parallel lines. For other angles of cut, closed figures (ellipse-like grain) are obtained. Hence, electron micrographs of overlapping crystals exhibiting moiré patterns often appear to be sculptures from wood. (See Fig. 5.)

VII. APPLICATIONS OF THE MOIRÉ TECHNIQUE TO PHYSICS

There are a number of problems in physics which can be solved by the moiré method. We have already alluded to some of them but now we shall be more specific.

The parallel line figures are representations of waves (actually square wave pulses), the wavelength being given by the interline spacing. If two waves of different wavelength are traveling in the same direction, one obtains a beat, the wavelength of the beat being given by eq. 3. If we have a collection of waves of slightly different wavelengths, we obtain a broad band called a wave packet.

If two waves of the same wavelength intersect at some angle θ they intersect at points along a line separated by a distance d given by eq. 1. With highly monochromatic parallel light as achieved with a laser one should also obtain interferences corresponding to $h + k = p$. (See Ref. 9.) This is Bragg's law for the first order diffraction of X-rays of wave length $\lambda = a$ by a crystallographic lattice of spacing d (in our formulation the angle is twice that chosen by Bragg). If we overlap three parallel line figures we can obtain a moiré pattern consisting of dots. This is analogous to von Laue's formulation of X-ray diffraction by a crystal. The moiré patterns obtained by the overlapping of the two gratings is also the solution of the modes (TE) in a rectangular wave guide used for microwaves (Ref. 9). The moiré lines represent the reflection boundaries of the wave guide. Since the moiré lines are perpendicular to the bisector of the angle between the waves (see Appendix A), the condition for reflection is satisfied. In Fig. 11 is shown the moiré pattern by the overlapping of No. 3 with its copy. The reflection condition is satisfied along any of the moiré lines. Thus the moiré technique can be used to design a microwave horn (Ref. 8).

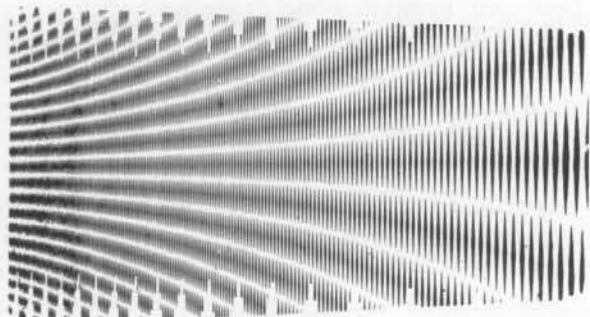


FIG. 11 Moiré patterns produced by the overlapping of No. 3 with its copy. This is the model for a microwave horn (ref. 8).

The interference of two spherical waves is represented by overlapping the equispaced concentric circles (No. 5). The resultant figures (hyperbolas) are those for the maxima and minima obtained in a ripple tank. In fact, it is the representation of the interference from two coherent (fixed phase) spherical waves, our figures being the two-dimensional Huygens constructions. Thus this represents the interference of light from two slits which have been illuminated by a common light source as in Young's experiment. It also represents the maxima and minima of the emission pattern from a pair of radio antennae which are emitting in fixed phase. When the center to center distances of the figures are within a distance less than the interline spacing, one observes a sharp highly directional line like a directional antenna. Drawing the centers apart weakens the beam and gives side bands like the side lobes in antennae patterns. The ellipses that are observed close to the centers correspond to the near-zone optical problem. (See Ref. 8.)

When three concentric circle figures are arrayed with their centers on a line one sees the breaking up of the hyperbolas into finer substructures. With more figures still further fine structure is observed. This illustrates the properties of a multislit system which for repetitive equispaced slits constitutes a diffraction grating. It is also analogous to a linear array of radio antennae.

A square array of concentric circles gives a moiré pattern similar to that of the far-field (Fraunhofer diffraction) image produced by a laser beam passing through an extremely fine mesh screen of round holes. The intersecting ellipses will appear with various overlapping orders. Patterns produced by laser beams passing through fine mesh screens can be explained in terms of overlapping equispaced concentric circles. (Ref. 8.) Such a diffraction system is a correct model for a square antenna array such as used for space tracking and radio astronomy.

The superposition of the equispaced circles (No. 5) and straight lines of the same spacing (No. 2) is the analog of the interference of a spherical wave and a plane wave. In optics this would be Gouy's experiment wherein the light (from a common point source) reflected from a plane mirror and a spherical mirror are made to interfere. Such interference would also occur with ocean waves (considered as plane waves) passing a small obstacle, such as a buoy, the obstacle then becoming a source of circular

wavelets. The resultant parabola can be altered in phase, that is, become dark or light, by slight movement of the circular pattern between a spacing of the line figure.

The combination of No. 5 and No. 2 represents a good approximation to diffraction (of the Fresnel type) past a straight edge, the tip of the edge being a source of spherical wavelets and we assume that the original source is far away and hence is represented by a plane wave falling on the straight edge. In this representation light beyond the tip of the straight edge is eliminated since this is the region of the geometrical shadow. This analogy also applies, of course, to sound waves where diffraction effects by obstacles are very common. By overlapping No. 2 on the combination of No. 5 with itself one obtains the diffraction pattern of a plane wave falling on a slit. An examination of the resultant moiré pattern suggests new features of the diffraction not heretofore treated in the optics literature (see Ref. 8).

Theory (and physical intuition) require that we must consider only the forward direction of the Huygens wave. To get a more detailed result, we must consider other points besides that at the tip of the obstacle as sources of secondary circular wavelets. Still higher degree of accuracy requires, as shown in advanced treatments of diffraction theory, a knowledge of the detailed nature of the straight edge. Nevertheless, our original combination (namely of No. 5 and No. 2) demonstrates the main features of diffraction about an edge. Similarly we can describe the features of diffraction by a slit by introducing another equispaced circular figure (No. 5), the slit width being given by the center to center distances of the circular figures. The complimentary obstacle, namely an opaque strip, is likewise described by this arrangement of figures. Light falling on a fine wire will exhibit interference fringes inside the geometrical shadow. The position of these fringes is given by No. 5 and No. 5 placed at the edges of the wire (*i.e.*, the same geometry as in Young's double slit experiment).

If a diffracting obstacle was illuminated by a source at some finite distance then we could consider the interaction of No. 5 placed with its center at the source and the edges of the diffracting plate would be secondary centers of light represented by No. 5. In all these diffraction problems the essential geometric parameter is the size of the diffracting object and the distances of the source and of the viewer taken relative to the wavelength of the light, that is, the spacing

of the lines of the figures.

Moiré patterns describe fields in two-dimensional potential problems. Such fields occur in electrostatics, magnetostatics, hydrodynamics, elasticity and gravity theory. Perhaps the most intuitive picture is given by fluid flow. The radial line pattern (No. 4) represents fluid emanating from its center and flowing uniformly outward across the surface, the lines representing the streamlines of flow. Since the lines do not indicate direction, the pattern could likewise be regarded as a sink in which liquid is flowing into its center. The greater the strength of the source (or the sink) the greater are the number of streamlines, and hence the smaller the angle separating them, since now the flux is greater. If the centers of the two figures (No. 4 and its copy) are brought close together, one has a source and sink combination. Liquid from one center flows into the other center. The path of the fluid (the streamlines) will follow coaxial circles, the centers of the circles lying on a line perpendicular to the line connecting the centers of the figures. When the figures are drawn apart one readily sees another moiré pattern between the two centers (Fig. 9B). The center of this moiré pattern corresponds to the stagnation point. Here two sources are pouring liquid toward each other and at the midpoint between the figures the liquid is stationary. Both types of moiré patterns are simultaneously visible at intermediate center to center distances. The two moiré patterns correspond to solutions of the Laplace equation in two dimensions. One could likewise show with other figures such as concentric circles with closer circles toward the center that the overlapping of the two figures gives two types of patterns. In molecular orbital theory these would correspond to the electron distributions for bonding and for antibonding atoms.

We can produce a stagnation point in another manner. Parallel straight lines represent streamlines of a flowing fluid. The smaller is the spacing the faster is the fluid flowing. To represent the flow of fluid past a source we superpose the straight line figure No. 2 on to the radial figure No. 4. Only one of the two stagnation points has physical meaning since we cannot specify in which direction the liquid is flowing.

Incidentally, the higher order but weaker moiré patterns which are seen are not mentioned in the hydrodynamic literature. You will notice that the moiré pattern also shows how the fluid flows about the source. This pattern represents

the resultant of two opposing movements of fluid. The variable spaced grating (No. 3) represents a fluid flowing in a straight line but with variable velocity, that is, it has a velocity gradient. The greater velocity is represented by the fine line portion of the screen. Place this figure over No. 4. The stagnation point is further from the center of No. 4, the coarser is the spacing in No. 3. In other words, the stagnation point becomes further from the center of the source the weaker is the oncoming parallel stream. If you measure the distance between the center of the radial pattern and the stagnation point you will find that it is proportional to the square root of the interline spacing of the parallel line figure. A source-sink combination when their centers are brought extremely close together is called a dipole or doublet. Smooth (potential) flow past a sphere can be represented by superposing the parallel line fig. No. 2 on to a doublet produced with No. 4 and its copy, the axis of the dipole being perpendicular to the direction of flow. You may be able to see in the moiré pattern a circle with streamlines produced about the dipole.

The coaxial moiré circles obtained by overlaying the radial figure on to its copy also represents the stress lines in a solid where the centers of the figures represent the locations of the application of the point stresses. Still further, it also represents the field lines about the poles of a horseshoe magnet as revealed by iron filings.

The moiré technique is very useful for mapping out two-dimensional fields in electrostatics. Conversion from two dimensional fields to three dimensional fields for a dipole is achieved by bending the print of No. 4 and overlaying with its transparency (for detailed discussion see Ref. 6). The radial line figure (No. 4) represents the field lines for a thin wire whose axis is perpendicular to the figure. We can determine, for example, the field lines for a vacuum tube by placing the figures at positions corresponding to the location of the electrodes in the tube, and the resultant moiré patterns describe the field. Linear fields are described by parallel lines. Since when one parallel line figure lies in the same direction ($\theta = 0$) as another, the resultant moiré fringes are perpendicular to the parallel lines ($\phi = 90^\circ$), this defines the requirement (the boundary condition) that at the surface of a conductor the field lines are perpendicular to that surface. We can represent the passage of field lines from a vacuum into a dielectric by placing the plane of a parallel line figure (either No. 1 or No. 2) out of the plane of a piece of white paper with the lines of the figure pointing downwards and casting a shadow of the figure on the paper. The shorter

the shadow the more the lines fan out, that is, the higher is the dielectric constant of the medium. A convergent lens placed on No. 2 corresponds to a sphere of higher dielectric constant than its surroundings. The variable line spacing figure (No. 3) represents a medium of variable dielectric constant, that is a dispersive medium. It is apparent, therefore, that by the judicious use of the figures one can represent any two-dimensional field problem and the moiré lines will give the exact solution of the problem. Electrical engineers might further note that the concentric circle figure (No. 5) represents the field lines about an electrically charged wire, the axis of the wire being perpendicular to the plane and passing through the center of the figure. The radial figure represents the end on view of a helical field so this figure can be used in certain problems associated with traveling-wave tubes used for microwave amplification.

The moiré effects corresponding to the distortion of an electric field produced by a medium of higher dielectric constant is more than a mere analogy. It can be used to measure an actual physical situation. When a ray of light enters a region of refractive index gradient, that is, a region where the optical dielectric constant varies with distance, the light ray is bent. The image of an equispaced parallel line figure whose lines are perpendicular to the direction of the gradient would be distorted. The greater the refractive index gradient the greater will the lines be displaced from their original positions. If we now superpose on the distorted image an equispaced parallel line figure the resultant moiré patterns will describe the actual refractive index gradient. (Ref. 10, see Appendix D.) This technique can be employed for the measurement of, for example, the diffusion of molecules in solution since the concentration is proportional to the refractive index of the solution and the refractive index gradient measured at various times can be related to the diffusion constant of the molecules. With some skill you can measure the heat waves about a hot body by this technique. Fold the woven screen in half and place a hot object (a soldering iron will do) between the folds which are in close register. You will see, by casting a shadow on a white wall, the refractive index gradient in the air produced by the hot object (see also Appendix D).

We can understand the produced moiré pattern by referring back to eq. 7. For nearly superposed parallel line figures (θ close to zero) the moiré fringe is turned more (that is, ϕ is greater) the closer the corresponding spacings are (that is,

the smaller is $|a-b|$ where b is the original spacing and a is the distorted spacing for the same indexed lines). Hence for closely registered figures in the undistorted regions the moiré fringes will be at right angles to the direction of the lines of the figure and for distorted regions at some smaller angle. In other words, the moiré fringes will deviate more or less from 90° the greater the difference of the spacings of the distorted and undistorted spacing. This idea can be utilized to demonstrate the conversion of a frequency modulated (FM) signal into amplitude modulation (AM). Imagine a parallel line figure where the spacings between the lines vary in some systematic manner. Then by placing upon it a uniformed spaced grating in close alignment the resultant moiré pattern will be a curve (the AM signal) which is the same function as the deviation (or distortion) function for the FM figure (see Appendix D).

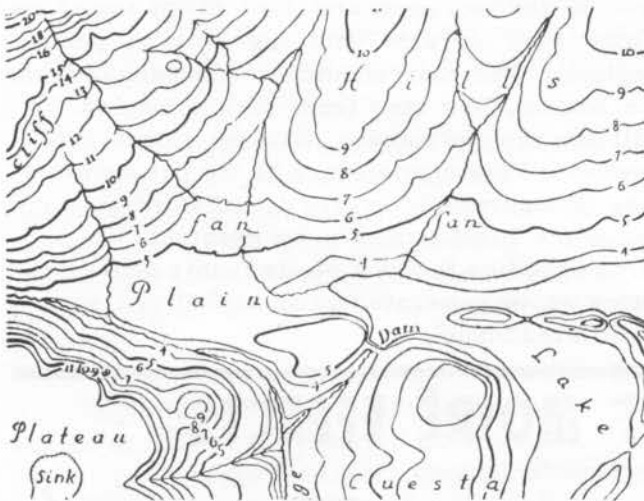


FIG. 12 A contour map (topological map) of a terrain (from E. Raisz, "General Cartography", McGraw Hill Book Co., 1948). Move the woven screen (No. 10) on the map and note the excitement particularly in the neighborhood of the gorge.

It is instructive to superimpose the woven screen over a topographical map (Fig. 12). The screen should be far enough away so that its spacing corresponds approximately to that of the closer contour lines of the map. In regions of greatest gradient, that is, the steepest descent in the mountains, the moiré lines will show a maximum. In this connection it is amusing to examine fingerprints through a grating. Using a stamp pad, make a fingerprint on a piece of white paper. Now overlay the print with No. 2. Note the moiré patterns. Each type of fingerprint displays a characteristic moiré pattern

as can be seen by examining Fig. 13 through the woven screen (No. 10). This might be a way of scanning large numbers of fingerprints in order to place them in different categories.

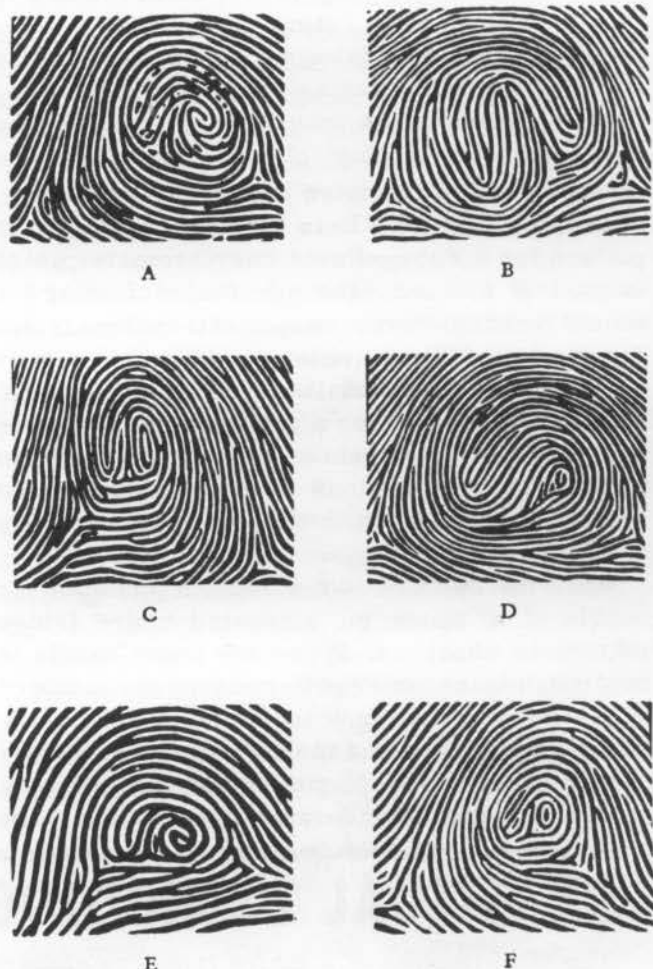


FIG. 13 Enlargement of representative types of fingerprints.

By permission from PRACTICAL FINGER-PRINTING by B. C. Bridges, Copyright, 1942, by Funk & Wagnalls Company, Inc.

Suppose that a flat ruling (or screen) is placed in contact with a curved reflecting surface. Then the shadow of the ruling would be superposed on the original ruling to give a moiré pattern which is a contour map of the curved surface. Place the halftone dot screen (No. 9) on the convex side of a teaspoon. Do you see the ovoid contour lines? The contour lines are larger if the grating No. 2 is used. Try this with a ping pong ball using strong illumination. One sees perfect circles. The moiré pattern constitutes a contour map of the sphere and hence is the same as No. 7. Try the woven screen (No. 10) held taut and just

touching the surface of an inflated rubber balloon. If we make the approximation discussed in Sec. VI, namely $ah \ll D$, the diameter of the spherical surface is $D = d^2/2h$ where d is the diameter of the moiré ring of order h (the center ring is $h = 1$, the second ring is $h = 2$, etc.) and a is the spacing of the ruling (or screen). This moiré pattern is analogous to Newton's rings obtained by illuminating with monochromatic light a plano-convex lens lying with its curved side on a reflecting glass plate. Note the similarity of this moiré pattern to the Fresnel zone plate (No. 6). It is also the same as the pattern for a Fabry-Perot interferometer which is part of a laser. The advantage of using the moiré technique over the optical technique is that for the latter a (the wave length of light) is several thousands times smaller than for the screens. As a consequence, for a given radius of curvature R the interference rings are usually of microscopic dimensions in the optical case but for the moiré method the rings are readily visible to the naked eye.

When the halftone dot screen is placed on the handle of a spoon an elongated moiré fringe pattern is observed. If now the spoon handle is bent slightly the moiré pattern changes considerably. Thus one can study the distortion of metals under a given load and thereby obtain the elastic moduli of the metal. Variations of this technique have been under considerable investigation these

past few years by mechanical engineers in order to determine the stress lines in objects subjected to various types of loading. For a comprehensive review (see Ref. 11). One simple procedure to study the stress properties of materials is to dip the woven screen (No. 10) in ink and impress it upon the sample. Now look through the woven screen held close to it. When the sample is under stress new moiré patterns will appear. It can be shown (Ref. 12) that the resultant moiré pattern is related to the stress tensors in the material. The question of distorted grids falls in the realm of non-Euclidean geometry and can be handled by the technique known as tensor analysis, a branch of mathematics which is very important in Einstein's General Relativity theory.

Two halftone screens, one of which is deformed, when placed in close register produce striking patterns. Crease or otherwise distort one of the screens and tape it on top of the undistorted screen with the dots in perfect register. The pair should be illuminated from the bottom. Now view from various angles. You will see rapidly moving patterns in the neighborhood of the distortion, with the patterns running most rapidly where the distortions, and hence the gradients, are the greatest. The patterns look like the bow waves from a ship or the shock waves generated by an airfoil in a supersonic wind tunnel.

VIII. VISUAL PSYCHOLOGY OF MOIRÉ EFFECTS

The visualization of a moiré fringe is closely tied in with the optics of vision. As we saw in Sec. V, for two overlapping gratings there are many points of intersection where a moiré fringe should appear but, in fact, we see only those corresponding to $h-k = p$. A hint as to what compels us to choose only one type of intersection comes from the illusion created at intersecting lines. Draw two straight lines which cross at some small angle. Note that at the intersection the lines appear pinched as though one had twisted two wires about each other. This effect is enhanced when viewing with red light and is least when viewing with blue light. Evidently it is connected with the inability of the eye to resolve the intersection. Many of the optical illusions, (notably the Poggendorf illusion (Fig. 14, compare Fig. 15), described in textbooks on psychology may be based on the phenomenon. Be that as it may, our eye is compelled to look across the intersection and this effect becomes more pronounced when we intersect many lines parallel

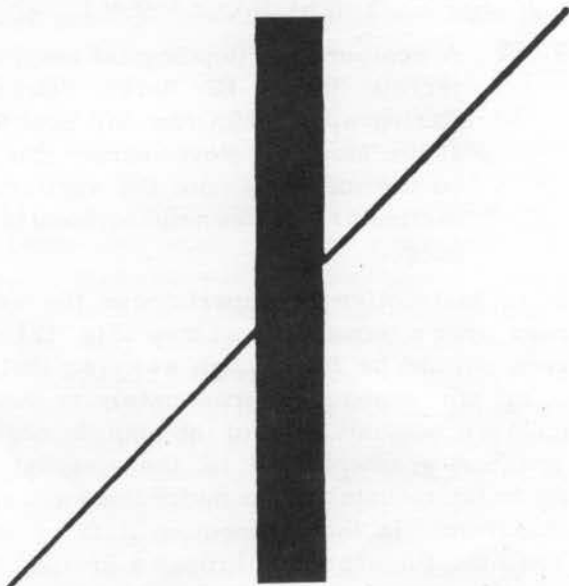


FIG. 14 The Poggendorf illusion. The thin line appears to be bent where it joins and leaves the thick line.

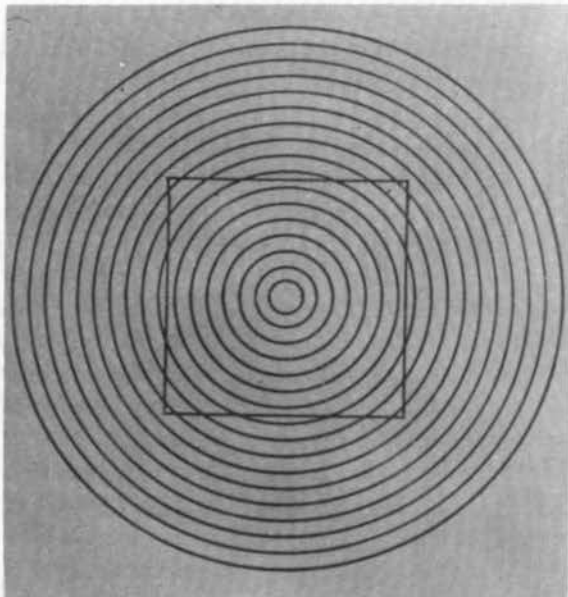


FIG. 15 The Orbison illusion. The square appears to bend inwards. The opposite effect is produced by drawing a square about the center of a radiating (spokes of a wheel) figure.

to the first two intersecting lines. Hence the eye which unconsciously searches the field will naturally tie together these points of intersection and we therefore see a moiré fringe. The illusion is less pronounced for lines crossing at larger angles and hence the moiré lines are unnoticed.

To see this effect of intersections in another way, lay a human hair on No. 2. You will see a series of dots at the points of intersection. If the hair is fine enough (red hair - natural, of course, is particularly good for this purpose) and the grating is held at arm's length, both the hair and the grating lines are too small to be resolved by the eye. Nevertheless, the points of intersection are readily visible. The intersection dots are further apart the smaller is the angle of intersection of the hair with the grating lines. In general, the distance between the dots is a direct measure of the first derivative (slope) of the curve which the hair describes. Conversely, for a dot distribution following a certain function, the curve of the hair is a solution of the first order differential equation.

The intersection effect can be demonstrated in another interesting way. Hold your finger an inch or so above the print of No. 3. In the coarser portions of the figure you will see an aura of bent lines close to the finger. This is the intersection of straight lines of the ruling with the diffraction fringes about your finger (see Ref. 8 for scientific applications of this phenomenon).

A wealth of data can be obtained by studying the single figures themselves. If the print of the radial pattern (No. 4) is held a distance less than the distance of normal reading (that is, less than about 10 inches) and viewed with one eye, a gray pattern is observed. This is the moiré pattern of No. 4 with its copy because a double image slightly displaced occurs due to the eye's inability to focus properly at short distances. If the same viewing is done with the print of the concentric circles (No. 5) radial moiré lines are observed. Obviously, persons with uncorrected astigmatism will see even more elaborate patterns.

View with both eyes open, either the radial line or the concentric circle print with its center close to your nose, you will see an overlapping of the figures, yet there is no moiré pattern to be seen for this stereoscopic condition. Each eye sees a separate image of the figure which is received by the brain but no physical overlapping of the figures occurs. As a consequence, no moiré pattern is produced. Overlapping figures produced by viewing a single figure through a calcite crystal, on the other hand, produces a moiré pattern (see Appendix E).

All sorts of interesting effects are observed by moving the single figures, preferably the prints. For example, if the coarse line figure (No. 1) is rocked back and forth a floating broken line runs through the figure while the other portions appear blurred. All the centro-symmetric figures, namely No. 4, 5, 6, and 7, show swirling arms when moved about rapidly with a circular motion. This is the superposition of the real image with the after-image which is momentarily retained on the retina of the eye. It is similar to the moiré pattern one obtains by superposing a figure with its copy, but now the pattern is moving with the frequency of the movement of the hand. An amusing effect is produced by moving the radial pattern (No. 4) with a back and forth linear motion. At right angles to the direction of movement a gray moiré pattern is observed and in the direction of movement the angles enlarge and contract.

Staring at the stationary single figures reveals considerable detail. For example, the radial figure (No. 4) shows moiré patterns in constant motion. Under strong white light illumination, gold and sometimes pink colors are seen. The inner circles of the concentric circle figure (No. 5) appear to be in rapid rotation. These effects are intimately tied up with the granularity of the retinal receptors (the cones of the fovea) and also with the rapid involuntary movements of the

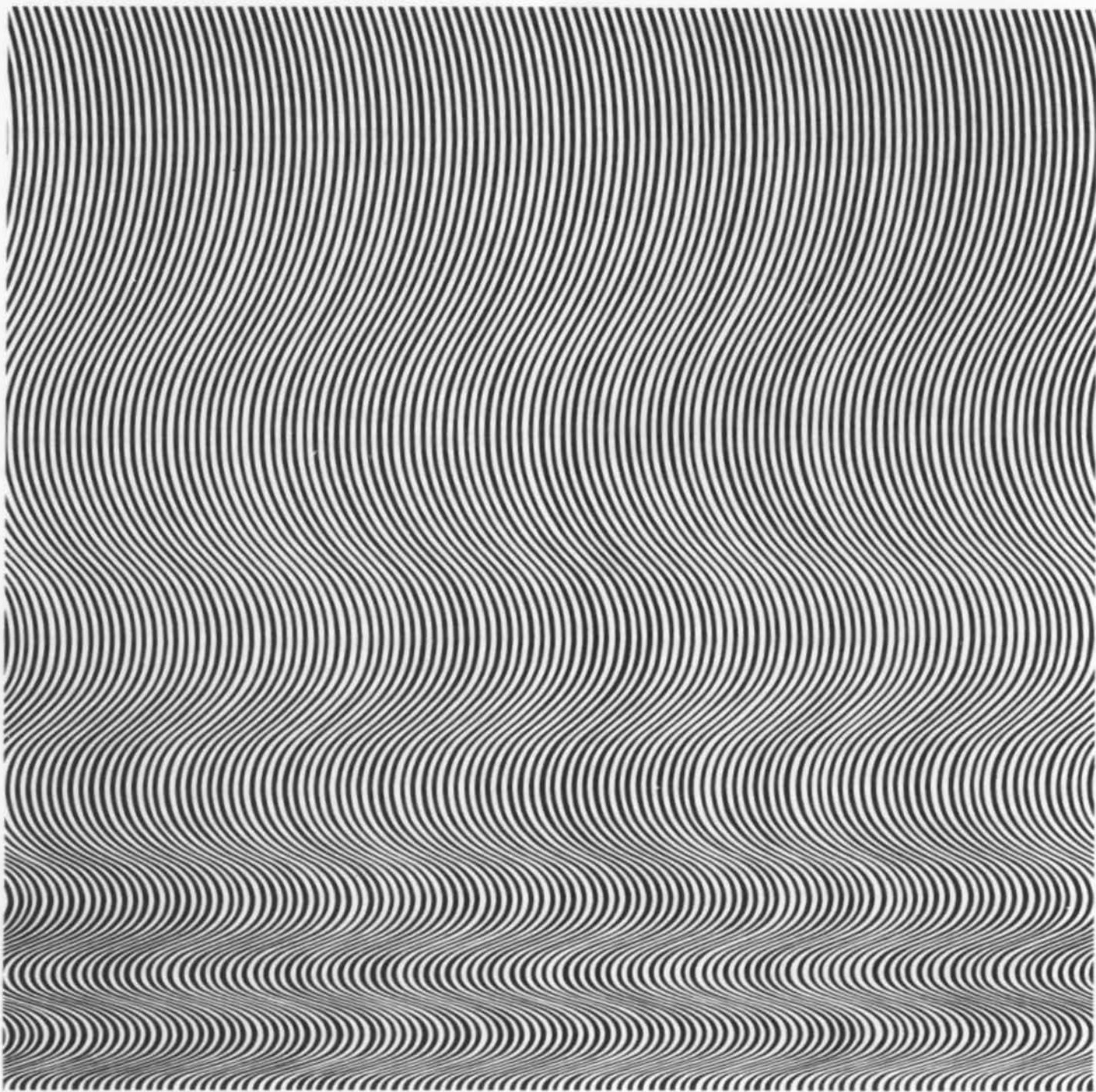


FIG. 16 "Fall" (1963) by Bridget Riley. (By permission of Gallery One). Note the rapid movements in the finer portions of the picture. Further startling effects are revealed by viewing the picture through the woven screen (No. 10).

eyeball (saccadic movements and tremors). Children see these effects readily while many adults may not. I have found, however, that artists (particularly those of the so-called optical school of painting) who are preoccupied with visual phenomena (for example, see Fig. 16) also see these effects without difficulty.

Still other subtle effects will be revealed to the patient viewer. For example, the coarse figure shows a cross-hatch of blue and yellow.

These are reminiscent of the colors of the brushes (Haitinger's brushes) which one sees by looking at the sky through a Polaroid dichroic filter. Even more subtle is the slow up-and-down movements of the reference peaks in No. 3.

Magnificent colored moiré patterns can be produced by overlaying colored figures (consisting of transparent colored lines on a clear background) on colored prints of the figures. A color moiré kit is now in preparation by the Edmund

Scientific Co. For example, a transparent figure consisting of yellow lines when placed over a blue on white print produces green moiré patterns because of the color subtraction effect. If you overlay the black lined radial transparency (No. 4) on the cover of the May, 1963 number of Scientific American, rich blue and red moiré patterns are produced. The colors appear deeper than the actual printed colored lines because the moiré effect isolates the colored lines from the white background which tends to dilute the strength of the colors of the individual printed lines.

The halftone dot screen (No. 9) is essentially a square-array coarse diffraction grating. When held close to the eye a distant light source appears as four light sources symmetrically arrayed around the original source. Look through the screen at some of the figures (notably No. 6) well illuminated and at several feet away. The figures now become beautiful colored designs.

APPENDIX A: Overlapping of Equispaced Gratings

We will now derive the equations given in Sec. IV for the overlapping gratings. Consider an enlarged region of Fig. 7.

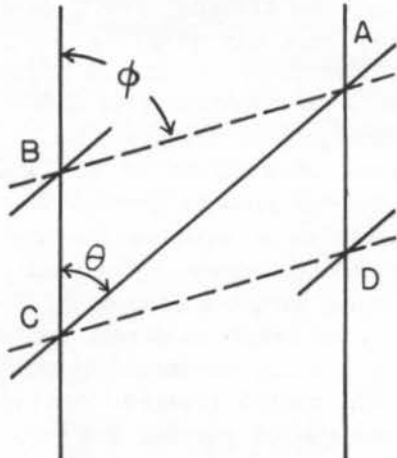


FIG. 17 An enlarged view of Fig. 7.

This is a parallelogram whose area ABCD equals (AB) times d or (AC) times a or (BC) times b, that is, the length of an edge times the perpendicular distance to the other parallel edge. We also have by the law of cosines that $(AB)^2 = (AC)^2 + (BC)^2 - 2(AC)(BC)\cos\theta$. Hence

$$\frac{1}{d^2} = \frac{1}{a^2} + \frac{1}{b^2} - \frac{2}{ab} \cos\theta$$

Solving for d we obtain eq. 5, namely

$$d = \sqrt{\frac{ab}{a^2 + b^2 - 2ab\cos\theta}}$$

A still more interesting view is seen by holding the transparency of the concentric circle figure (No. 5) with its center close to the eye and move the center of the figure about with a slow small circular motion. Solid objects appear to be alive. The effect is particularly beautiful when viewing flowers, such as chrysanthemums. The impression is one of an underwater scene of hydra with moving tentacles. These few examples suffice to give the reader some idea of the fascinating possibilities of viewing the world through repetitive figures. It is conceivable that the fovea of the eye acts as an almost imperceptible circular figure superposed on our vision (certainly its histological structure would not rule out this possibility) but we are too accustomed to its presence to notice it. Apparently it takes a van Gogh to reveal to us the existence of this subconscious figure.

When θ becomes small, $\cos\theta$ is approximately unity, in which case the denominator becomes $a - b$ and hence we obtain eq. 3.

For the special case of $a = b$, eq. 5 becomes

$$d = \frac{a}{\sqrt{2}\sqrt{1-\cos\theta}}$$

This is the same as eq. 1 since

$$\sin\theta/2 = \sqrt{(1-\cos\theta)/2}$$

From the law of sines, we see from the above drawing (from B drop a perpendicular to CD and another to AC)

$$\frac{d}{\sin\theta} = \frac{a}{\sin\theta}$$

Inserting d from eq. 5 and solving sin we obtain eq. 4, namely

$$\sin\theta = \frac{b\sin\theta}{\sqrt{a^2 + b^2 - 2ab\cos\theta}}$$

By using the theorem of Pythagoras and the definition of the sine we can also express this in terms of the slope of the moiré fringe, namely

$$\tan\theta = \frac{b\sin\theta}{(a^2 + b^2 - 2ab\cos\theta) - b^2\sin^2\theta} = \frac{b\sin\theta}{a - b\cos\theta}$$

For the special case of $a=b$ the above equation becomes

$$\tan \phi = \frac{\sin \theta}{1 - \cos \theta} = \frac{2 \sin \theta / 2 \cos \theta / 2}{2 \sin^2 \theta / 2} = \cot \theta / 2$$

and eq. 4 becomes

$$\sin \phi = \frac{\sin \theta}{\sqrt{2 \sqrt{1 - \cos \theta}}} = \frac{2 \sin \theta / 2 \cos \theta / 2}{2 \sin \theta / 2} = \cos \theta / 2$$

which is eq. 6. That is, for $a = b$, ϕ is 90° plus

APPENDIX B: Focal Length Determination

As mentioned in Sec. IV, the focal length of a lens can be determined by the moiré technique. In this appendix the relation between the focal length of a lens and the changes in the moiré pattern caused by the lens will now be considered. In particular we shall derive equation 8 of section IV.

Suppose that a grating of equispaced lines of spacing a is overlapped at an angle θ with an identical grating which is separated by same distance. Imagine that the system is illuminated with a parallel beam of light. Then the angle ϕ which the moiré fringes make with the y -axis is given by eq. 6, namely that the sine of ϕ equals the cosine of $\theta / 2$. Now interpose a lens between the two gratings. The lens will now make the apparent spacings (b) of the grating different from a . The fringe angle is now governed by eq. 4, i.e., $\sin \phi$ for a different from b . For our purposes it is more convenient to describe ϕ in terms of the equivalent expression (derived in Appendix A)

$$\tan \phi = \frac{b \sin \theta}{a - b \cos \theta}$$

or

$$\frac{a}{b} = \frac{\sin \theta}{\tan \phi} + \cos \theta = \frac{\sin \theta + \cos \theta \tan \phi}{\tan \phi}$$

Now multiply the numerator and denominator by $\cos \phi$, and recalling that $\sin(u+w) = \sin u \cos w + \sin w \cos u$, we obtain

$$\frac{a}{b} = \frac{\sin \theta \cos \phi + \cos \theta \sin \phi}{\sin \phi} = \frac{\sin(\theta + \phi)}{\sin \phi}$$

If the second grating is at a distance s from the lens and this distance is less than the focal length f of the lens than the ratio of b and a (the magnification factor) is shown from elementary ray tracing to be

$$\frac{f - s}{f} = \frac{b}{a}$$

$\theta / 2$ or, in other words, the perpendicular to the moiré line bisects the angle θ .

Alternatively, we could have derived these equations by the indicial equation technique by eliminating h and k from the following equations:

$$x = bh \text{ (the equation for the vertical lines)}$$

$$x \cos \theta - y \sin \theta = ak \text{ (the equation for the inclined lines)}$$

$$h - k = p \text{ (the indicial equation)}$$

Note that the difference, $b-a$, relative to a is s/f . Rearranging this equation we obtain

$$f = s \frac{1}{1 - b/a}$$

Introducing the relation involving θ and ϕ above, we obtain eq. 8, namely

$$f = s \frac{\sin(\theta + \phi)}{\sin(\theta + \phi) - \sin \phi}$$

This expression is for a convergent (e.g., plano-convex) lens and results in a clockwise rotation of the moiré fringes relative to the background fringes. For a divergent (e.g., meniscus) lens $\sin(\theta + \phi)$ is replaced by $\sin(\phi - \theta)$. The resultant moiré fringes are now turned in a counterclockwise direction relative to the background fringes. Eq. 8 shows that the amount of rotation of the moiré fringes caused by the lens is greater for smaller θ .

We could have avoided the use of parallel light by photographing, by contact printing, the first grating with the lens on it. Then on placing this photograph in direct contact with the unaltered grating we would observe the rotation of the moiré fringes. Another arrangement consists of placing the lens beyond the two separated gratings rather than between them. This would require the use of another lens formula in the calculations.

While we are on the subject of lenses, it might be pointed out that the Fresnel zone plate (No. 6) can act as a lens. This rather unexpected phenomenon served as the most dramatic proof of the Fresnel theory of the wave nature of light. The zone plate describes the resultant amplitude at a given point due to the wave front from a distant source. As a consequence, the zone plate is capable of producing images like a lens. In fact, in conjunction with a low-powered eyepiece the zone plate can be used as a telescope. It has two drawbacks, however: firstly it has a very

long focal length. The principal focal length f is given by $f = r^2/\lambda$ where r is the radius of the inner ring of the figure and λ is the wavelength of light. For, No. 6 $r = 0.5$ cm and if we take bluish-green light ($\lambda = 5000$ Angstroms $= 5 \times 10^{-5}$ cm.), then $f = 5 \times 10^3$ cm $= 50$ meters. By photographic reduction of the figure by, say, a factor of ten we can reduce the focal length to a more reasonable value (50 cm. in this example). By carrying out this reduction in size, however, we have introduced a second disadvantage of the zone plate focusing technique. The outer circles of the

figure become so close that they serve as a diffraction grating. As a consequence, the focused image is colored, unless, of course, we are using monochromatic light.

The essential advantage of the zone plate method is that focusing takes place without refracting (or reflecting) materials. Indeed, microwaves have been focused with zone plates consisting of large metal rings. In principle, X-rays could be focused by this means if there were some way of making an extremely minute zone plate.

APPENDIX C: Theory Of The Screen Determiner

In this book we have considered various ways in which the moiré technique is employed to determine the spacing of a periodic structure such as a screen or an equispaced grating. Thus in Sec. IV we showed that by overlaying the periodic structure with an equispaced grating whose spacing is comparable with the spacings of the structure we could determine the spacings of the periodic structure. The spacings would be calculated from the beats (eq. 3), from the fringe spacings (eq. 5 at θ different from zero), or from the inclination of the fringes (eq. 4). A direct determination of spacing is obtained by overlaying with the logarithmic spaced grating (No. 3) and no calculation is required as long as one knows the spacing frequency distribution of the variable spaced figure.

A more useful figure for direct spacing determination is a fan (Fig. 18). This is constructed by connecting equispaced points along a line to a common origin which lies on the axis perpendicular to the line. At a distance c from the origin, the value of x (the horizontal distance) is less than ha by some length δ , i.e., $x = ha - \delta$. By elementary geometry we see that $\delta/ha = y/c$ and hence $x = ha - y/c = ha(1 - y/c)$, which is eq. 22.

We now overlay the fan with an equispaced grating of spacing a with the lines running along the y -axis of the fan (i.e., $x = ka$). Solving for h and k and substituting into the indicial equation $h - k = p$ we obtain

$$\frac{x}{a} \frac{1}{(1-y/c)} - \frac{x}{a} = p$$

or, on rearrangement

$$y(x+pa) = cpa$$

These are rectangular hyperbolas (see Fig. 19). The asymptotes of the hyperbola occur where the spacing of the grating exactly matches the spacings of the fan. In other words, we obtain a beat at infinity when the grating spacing matches the spacing in the x direction of the fan. In the Edmund screen determiner, the spacings (as lines per inch) are marked along the fan.

The moiré pattern for two overlapping fans with their origins in opposite directions is of some interest. The equations for the two identical fans are $x = ha(1 - y/c)$ and $x = ka(1 + y/c)$, respectively. These equations together with the indicial equation gives

$$\frac{1}{1-y/c} - \frac{1}{1+y/c} = pa/x$$

For c much larger than y , i.e., taking that part of the fan close enough to the origin, and making the approximations $(1-u)^{-1} = 1+u$ and $(1+u)^{-1} = 1-u$ for small u , we obtain

$$xy = 1/2 cpa$$

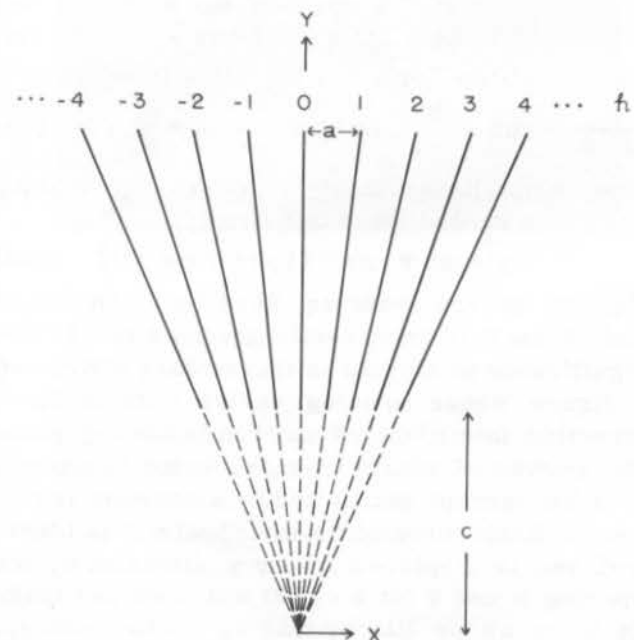


FIG. 18 A fan.

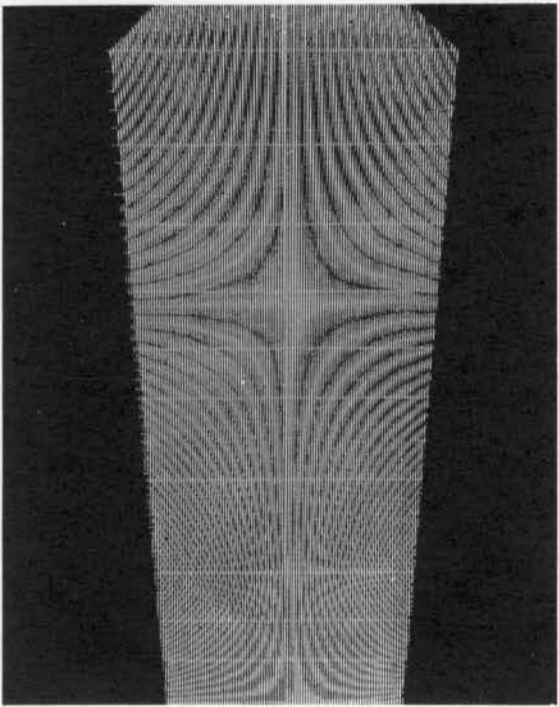


FIG. 19 Screen determiner with No. 2 superposed.

This is a series of rectangular hyperbolas which become progressively closer as one moves outwards at 45° from the axes of the figure. If we regarded the figure as a contour map, the 45° degree line would represent the line of steepest descent, the origin being the lowest point.

There is another way of producing rectangular hyperbolas by the moiré technique. Thus if an equispaced grating of spacing b is superposed on equispaced concentric circles of spacing $\sqrt{2}b$, one obtains rectangular hyperbolas but now the hyperbolas are equally spaced along the line 45° to the axes of the hyperbolas. That rectangular hyperbolas are formed in this manner can be seen from eq. 12 which on substitution of $a=\sqrt{2}b$ gives an equation of the form $x^2-y^2=c$ (c is a constant). On rotation by 45° one obtains the ordinary formula for rectangular hyperbolas, namely, $2xy=c$. Rectangular hyperbolas can be demonstrated by holding No. 5 sufficiently far above No. 2 so that apparent spacings of No. 5 are 41% greater (note: $\sqrt{2}=1.41$) than the spacings of No. 2.

APPENDIX D: Overlapping On To Variable Spaced Grating

The overlapping of an equispaced grating on to a variable spaced grating has considerable importance in experimental physics. Suppose that each line of the variable spaced grating is located at a distance $f(hb)$ from a corresponding position hb of an equispaced grating of spacing b . In other words, the equispaced $x=hb$ is modified by the function $f(hb)$. Hence the equation for the variable spaced grating is

$$x = hb + f(hb) \quad (i)$$

Now we overlap this figure with an equispaced grating of spacing a so that the equation for this second figure is

$$x \cos \theta - y \sin \theta = ka \quad (ii)$$

The indicial equation for the resultant moiré pattern is $h-k=p$ or

$$h=k+p = \frac{1}{a} (x \cos \theta - y \sin \theta) + p \quad (iii)$$

Substituting eq. iii into the first equation yields

$$x = pb + \frac{b}{a} (x \cos \theta - y \sin \theta) + f\left[pb + \frac{b}{a} (x \cos \theta - y \sin \theta) \right] \quad (iv)$$

We can simplify this expression by referring the system to new (primed) axes obtained by a

rotation in a clockwise direction by an angle θ , using the standard rotational transformation equations

$$x' = x \cos \theta - y \sin \theta \quad (v)$$

$$y' = x \sin \theta + y \cos \theta \quad (vi)$$

$$\begin{aligned} \frac{y}{\sin \theta} &= pb + \left(\frac{b}{a} - \cos \theta \right) x' + f\left(pb + \frac{b}{a} x' \right) \quad (vii) \end{aligned}$$

The term linear in x' is removed by making $b=a \cos \theta$ so that we obtain finally

$$y' = \csc \theta [pb + f(pb + \cos \theta x')] \quad (viii)$$

Eq. viii differs from eq. 33 of Ref. 6 in that in Ref. 6 $\csc \theta$ is incorrectly given as $\sec \theta$. The significance of eq. viii is that we have converted a figure whose spacing varies only in the x direction into a moiré pattern in the $x-y$ plane the curves of which have the same functional relation (except multiplied by a constant factor $\cos \theta$). Each curve of the moiré pattern is identical and is displaced in the y direction by the spacing $b \csc \theta$ (or $a \cot \theta$) which we can make as large as we like by making θ small enough. For small values of θ eq. viii gives for the zero moiré line (note: for θ small $\csc \theta \rightarrow \theta^{-1}$, $\cos \theta$

$$\longrightarrow 1, x' \longrightarrow x, \text{ and } y' \longrightarrow y) \text{ simply}$$

$$y/\theta = f(x) \quad (\text{ix})$$

that is, the original spacing function.

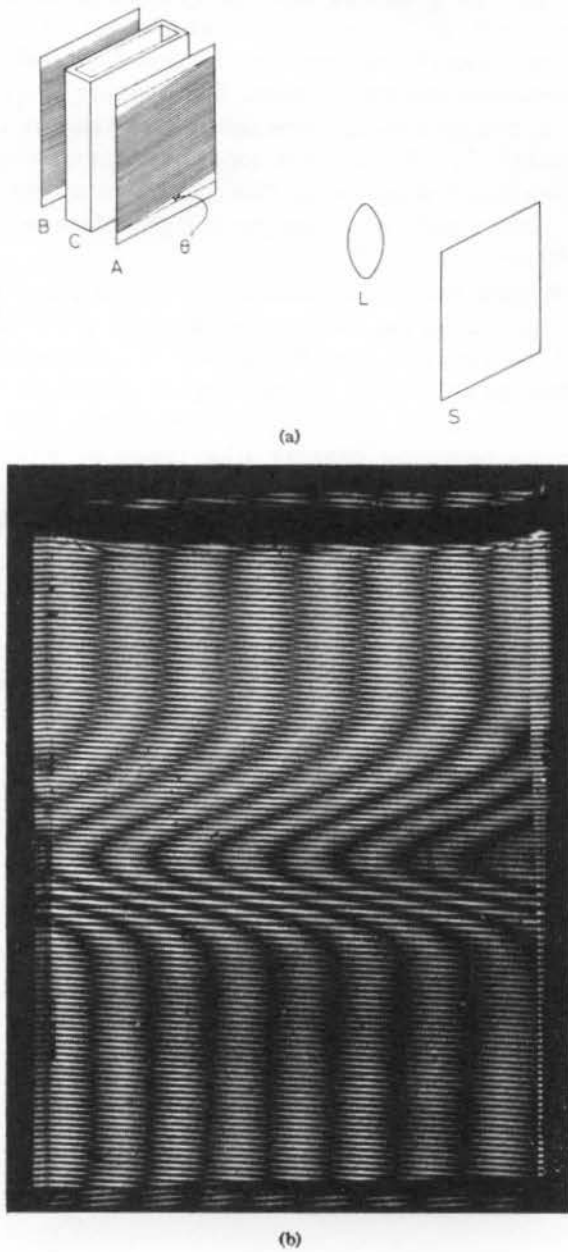


FIG. 20 (a) Diagrammatic sketch of diffusion apparatus. (b) Moiré pattern formed on the screen (S) in sketch (a). Cell C thickness 1 cm.; spacing of the ruling (B) 0.2 mm.; angle θ of ruling (A) 5° ; focal length of lens (L) 150 mm. Diffusion curve for aqueous solutions of 60% glycerol against 50% glycerol. (from ref. 10).

In Fig. 20a is shown an experimental arrangement for studying the diffusion of molecules where the diffusion is taking place in the vertical

direction (here taken as the x-axis). The spacings of the equispaced grating B will appear to be non-uniform due to the refractive index gradient in the diffusing system C, the displacements from the original positions being greatest where the gradient is the greatest. Our problem is to determine the function governing these displacements. On observing the distorted image with another equispaced grating A we obtain the moiré patterns shown in Fig. 20b (the y-axis is taken in the horizontal direction). These are Gaussian error curves. If we had studied the diffusion of a concentrated solution against water (e.g. pure glycerol overlayed with water) we would have obtained a skewed moiré pattern with its skewness in the direction of the water layer. In this case the initial boundary would be very sharp but after a few hours of diffusion the skewed gradient curve would become apparent. The integral of the concentration gradient, that is, the concentration at all positions in the diffusion cell, may be obtained in a direct manner by the moiré technique using a prismatic diffusion cell rather than a cell of rectangular cross section (Ref. 13).

Other arrangements of the gratings have been considered (Ref. 6). For example, both gratings can be placed on one side of the cell (at positions A and S of Fig. 20a). One can measure extremely small refractive index gradients by projecting an image of grating B on to grating A of Fig. 20a. By such an arrangement one can readily study thermal gradients about a hot object and hydrodynamic or aerodynamic flow patterns about an object. Incidentally, if white light is used the moiré lines will appear colored due to chromatic aberration of the projector lens.

When a diffraction image is examined with an equispaced grating whose spacings are comparable to some of the diffraction line spacings a moiré pattern is produced (Ref. 8). The moiré curve determines the functional relation of the spacings in the diffraction image. Furthermore, due to the magnification effect of the moiré phenomenon, diffraction lines which are very close together, and therefore poorly resolvable, are now discernible. The same technique can be used to resolve the fine structure in the band spectra of molecules and thereby effectively increase the resolution of a spectrograph.

APPENDIX E: Experiments With Calcite Crystals

There are some moiré effects with calcite crystals which illustrate the power of the method in its application to optical crystallography. Calcite (also called Iceland Spar) occurs naturally in the form of rhombs with edge angles of 102° and 78° . Light passed through the parallel faces of the crystal is refracted into two beams. Place the crystal over a spot on a piece of paper. The spot appears as two spots. When the crystal is rotated one spot remains stationary (formed by the ordinary ray) while the other spot (formed by the extraordinary ray) moves around the stationary spot. The line connecting the two spots passes along the optic axis of the crystal and is in the direction of the obtuse vertex of the rhomb. The two rays are polarized at right angles to one another as can be seen by rotating a Polaroid dichroic filter on the double spot image and noting the disappearance of one or the other spot.

When the calcite crystal is placed over any of the centrosymmetric figures (No. 4, No. 5, or No. 6) one observes moiré patterns as gray lines. These are the moiré patterns produced by the figures and their copies with their centers being slightly displaced. Applying the Polaroid over the moiré pattern destroys the pattern and only the single figure is observed.

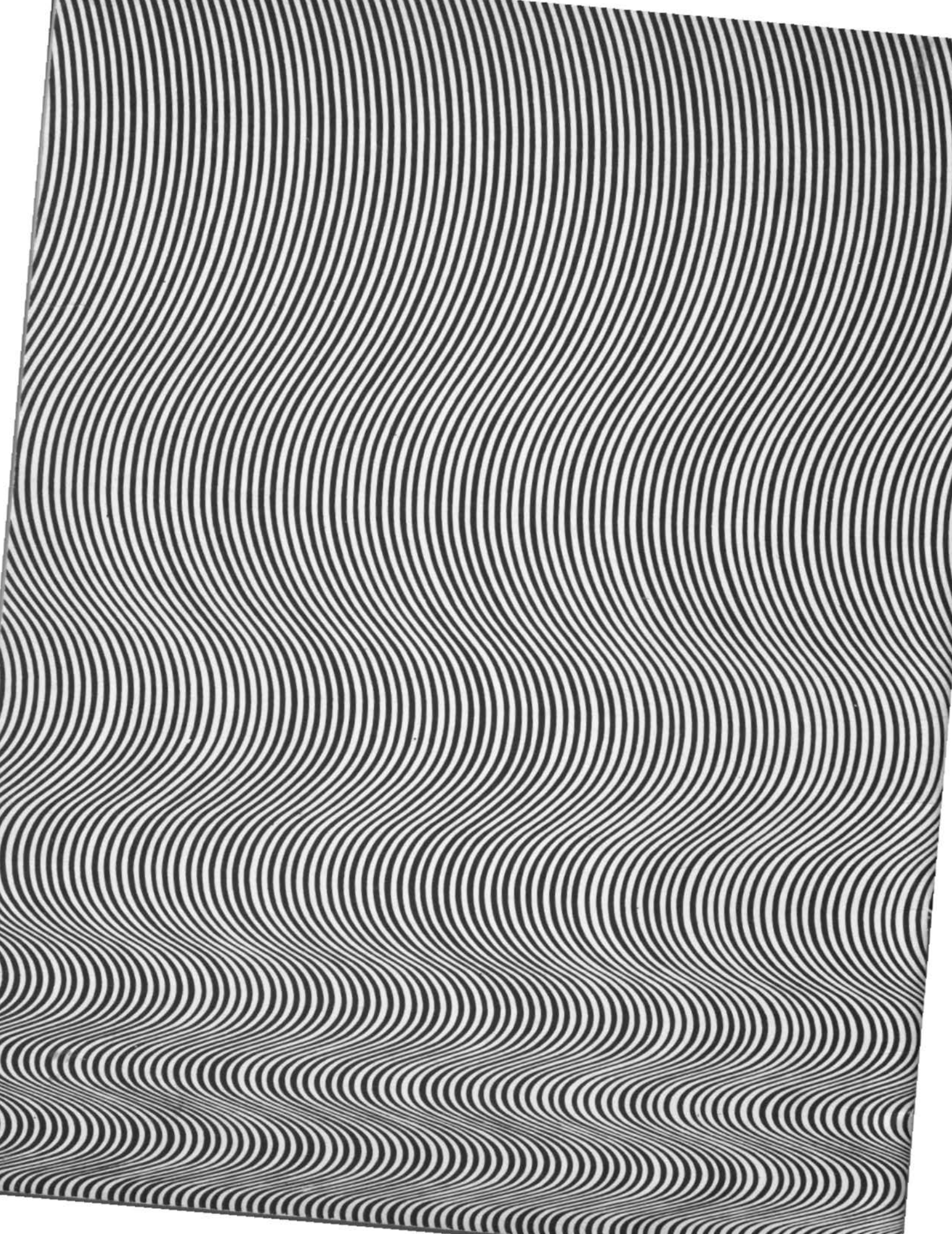
If the calcite crystal is placed between two equispaced gratings and the system is illuminated (from underneath) with white light, strongly colored moiré fringes are observed. In only one orientation, namely, when the grating lines lie along the optic axis, are the moiré fringes free of color. In other orientations the colored fringes indicate the dispersion (the variation of refractive index with wave length of light) of the extraordinary ray.

When a calcite crystal is cut into a plate with its optic axis parallel to the surface of the plate and viewed between Polaroids, the illumination being provided by a convergent beam of light (the so-called conoscopic condition), one observes patterns exactly like those of Fig. 19. These curves are the curves of equal optical path difference (equal retardation) between the ordinary and extraordinary components. The wavelengths (inversely proportional to the refractive index) of the extraordinary waves are different for different directions of propagation of light through the crystal, whereas the wave length for the ordinary waves are the same for all directions of transmission. The mathematical analysis for this optical problem then follows the same analysis as that given in Appendix C.

FOR YOUR NOTES:

REFERENCES

1. J. Guild "The Interference Systems of Crossed Diffraction Gratings", Oxford University Press (1956).
2. J. W. Menter, "The Electron Microscopy of Crystal Lattices", Advances in Physics, 7, July (1958). See especially pages 328-348.
3. G. Oster and Y. Nishijima, "Moiré Patterns", Scientific American, 208, May, 1963, pp. 54-63.
4. J. Guild, "Diffraction Gratings as Measuring Scales", Oxford University Press, 1960.
5. R. V. Jones and J. C. S. Richards, "Recording Optical Lever", Journal Scientific Instruments, 36, pp. 90-94 (1959).
6. G. Oster, M. Wasserman, and C. Zwerling, "Theoretical Interpretation of Moiré Patterns", Journal Optical Soc., Amer. 54, pp. 169-175. February, 1964.
7. G. Edgecombe, "Moiré Bands", Mathematics Teaching (Bulletin Assoc. Teachers of Math., Great Britain) No. 26, Spring 1964.
8. G. Oster, "Representation and Solution of Optical Problems by Moiré Patterns", Symp. on Quasi-Optics, Polytechnic Institute of Brooklyn Press (1964). Distributed by Wiley-Interscience, New York.
9. J. A. Giordmaine, "The Interaction of Light with Light", Scientific American, 209, April, 1964, p. 45.
10. Y. Nishijima and G. Oster, "Moiré Patterns: Their Application to Refractive Index Gradient Measurements", Journal Optical Soc. Amer., 54, pp. 1-5, January, 1964.
11. P. S. Thescraris, "Moiré Fringes: A Powerful Measuring Device", Applied Mechanics Review, 15, 333 (1962).
12. R. M. Bromley, "Two-dimensional Strain Measurements by Moiré", Proceedings Phys. Soc., 69B, 373-381 (1956).
13. C. J. van Oss, "The Use of Gratings Producing Moiré Patterns for Measuring Refractive Index Gradients", Journal Scientific Instruments, 41, pp. 227-228, April, 1964.



NEW -- MOIRÉ PATTERNS



Revolutionary New Scientific Tool!

Moiré patterns have for a long time been an overlooked and underdeveloped scientific, artistic and decorative tool. Here is a scientific advance of extreme importance as has been shown by Dr. Gerald Oster of Brooklyn's Polytechnic Institute. Ever since the historic article by Oster and Nishijima, in a recent issue of "Scientific American," scientists and the scientifically inclined throughout the world have been discussing the subject with rabid interest and excitement.

Moiré patterns are the predictable patterns reproduced as a result of interference beats between two regular patterns (parallel and equispaced lines for example). While the phenomenon has been known for years, Professor Oster has developed the whole subject into a basic scientific tool, and an explainable art form.

Though beautiful in themselves, and a joy to work with, moirés have important and significantly profitable applications as described below. It is with great pleasure that we are now able to offer Dr. Oster's book on moiré patterns along with experiment kits designed to his specifications.

Mr. Edmund Forecasts:

Within a few years, products and objects of art and design utilizing these principles will be generating

millions of dollars of sales volume. The study and utilization of Oster-Moiré Patterns is an overlooked-underdeveloped field; those who experiment with and apply these will make many new, fascinating and profitable discoveries.

Moirés Offer You Fantastic Opportunities:

✓ Inexpensively Measure One Part in Billion

The combination of a grating and a front-surface mirror, one of the most sensitive physical devices known, is capable of measuring extremely minute angular differences.

✓ Solve Problems in Physics

Measure the diffusion of molecules in solution or the heat waves around a hot object by refraction.

✓ Reproduce Math Concepts VISUALLY

Moirés, many actually provide visualizations of math concepts themselves, offer a convenient method of producing projections of any intersecting structures.

✓ Experiment With a Whole New Art Medium

See bottom of page. Moirés can also be used to analyze the basic colors used in original paintings and reproductions.

SEE DR. OSTER'S BOOK AND EXPERIMENT KITS . . . PAGE 74



"Moiré sculpture called 'The Fountain' is examined by Professor Gerald Oster. It is made of stainless steel and revolves to generate patterns." New York Daily News Photo.

✓ Investigate "Lensless Optics"

✓ Excellent Science Fair Project

Most of Dr. Oster's theories require only a knowledge of high school mathematics and can be employed as the heart of or the dramatization of hundreds of projects.

✓ Opens Up Whole New Field of Psychology

Many of the optical illusions described in psychology text books may be based on moiré phenomena.

✓ Study Liquid Flow And Stress Lines

In hydrodynamics, moirés give an extremely precise picture of fluid movement. With them you can also study the distortion of metals under a given load and obtain the elastic moduli of the metals.

"Moving Art Points Way For Science"

reads N. Y. Sunday News headline

We quote from the article. "Many artists involved in avant garde sculpture will be surprised to hear they are intuitive scientists." It seems their motor-driven sculptures create shimmering geometrical patterns while in motion, patterns which can solve problems in theoretical physics, aerodynamics and other computations, according to a Brooklyn professor.

These designs generated by the moving sculpture are called Moirés by Dr. Gerald Oster of Polytechnic Institute of Brooklyn.

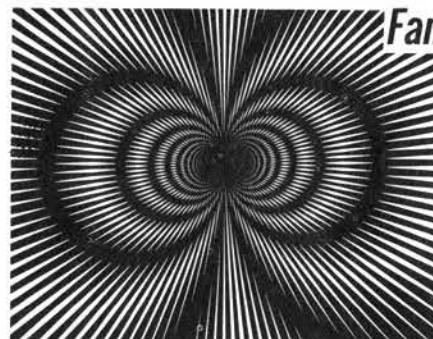
You might call a moiré an optical illusion. An object in motion such as the mobile sculpture produces the effect of overlapping lines or curves forming designs from light reflected on the moving surfaces. This was demonstrated by the professor at a press conference . . . held around a Manhattan exhibit of "Kinetic Sculptures" at the Howard Wise Gallery, 50 W. 57th St. (New York)

"Many of these exhibits are based on the moiré phenomenon," he said, standing before one of whirling steel fronds titled "Fountain," by Len Lye.

"While artists have been intuitively using the moiré principle, as they become more aware of what it offers, their creative possibilities are enormously increased."

MOIRÉ PATTERNS OFFER AN EXPLOSIVE NEW FIELD OF INVESTIGATION

NEW -- MOIRÉ PATTERNS



Fantastic New Opportunities !!

EXPERIMENT WITH MOIRÉ PATTERNS

JUST IMAGINE . . .

- Inexpensively measure one part in billion
- A whole new art medium
- Reproduce math concepts VISUALLY
- Solve problems in physics
- Investigate "Lensless optics"
- Visually study liquid flows and stress lines in objects
- Excellent Science Fair project
- So amazing it opens whole new field of visual psychology
- Fascinating Fun to experiment with

"THE SCIENCE OF MOIRÉ PATTERNS" BOOK

By Dr. Gerald Oster, Polytechnic Institute of Brooklyn. Written exclusively for Edmund Scientific Co., this new and authoritative book introduces you, through experiments, to the exciting world of moiré. You need only an understanding of high school mathematics to enjoy it. And the experiments require only the materials listed in the following kits. Here is a book that belongs in every high school and college library. Typical chapter headings: Moiré Patterns in Everyday Life, The Moiré Kit, Seeing Moiré With Screens, General Approach, Interpretation of Moiré Patterns in Terms of Projective Geometry, Visual Psychology of Moiré Effects, etc. 32 pages (8½" x 11"). 25 illustrations and diagrams.

No. 9068 \$2.00 Postpaid

STUDENT'S AND EXPERIMENTER'S MOIRÉ KIT

Includes the 8 designs as described. They are produced on clear acetate, 3/4" x 4" (.005" thick) and again on white Kromekote paper (coated one side) 3/4" x 4 1/2" (.010" thick). Kit also includes one piece of 3/4" x 4", 150-dot halftone screen on film; and the text "The Science of Moiré Patterns".

No. 70,718 \$6.00 Postpaid

As above, but without text. No. 60,462 \$4.00

EDUCATOR'S AND DESIGNER'S MOIRÉ KIT

Includes the 8 basic designs as described, but produced on .020" thick acetate and .012" Kromekote (coated both sides). These heavier sheets are much more durable for classroom and everyday use. Also included are: two pieces of 3/4" x 4", 150-dot halftone screen on film; 1 piece, 8" x 10 1/2" of 20 mesh woven fiberglass screen; and the text "The Science of Moiré Patterns". Complete kit. No. 70,719 \$8.50 Ppd.

As above, but without text. No. 60,464 \$6.50 Ppd.

MOIRÉ PATTERN ACCESSORY KIT

Use with either kit above to perform additional experiments described in Dr. Oster's text. Contains: balloon (approx. 12"); 1 each, 133 and 150-line Ronchi rulings on film; one-way mirror (on film); transmittance and reflective diffraction gratings; red and blue filters; polarizing film; front surface mirror; cylindrical lens; plano convex and negative lens; 1 piece calcite.

No. 60,487 \$8.00 Ppd.

EDMUND HALFTONE SCREEN DETERMINER

For moiré experiments and graphic arts. Double-sided. Simply place one side over halftone reproductions to accurately and quickly identify number of lines per inch (50 to 200). Also has inch, mm, agate and pica rules. Reverse side measures percentage of stereotype shrinkage for any newspaper halftone, plus screen angles for color reproductions. Durable plastic sheet, 5" sq. No. 40,751 \$2.25 Ppd.

READ MORE ABOUT MOIRÉ PATTERNS ON PAGE 38 . . . RONCHI RULINGS, PAGE 75, CAN ALSO BE USED FOR MOIRÉS

IMPORTANT NOTICE

Don't Overlook the Moiré Pattern Accessory Kit

In line with our policy of bringing you scientific items at low cost, we draw your attention to the Moiré Pattern Accessory Kit. The Student's and Experimenter's Kit and the Educator's and Designer's Moiré Kit enable you to perform most of the experiments set forth in Gerald Oster's text. However, in order to perform all of the experiments, to follow all of the arguments, you will want to order the Moiré Pattern Accessory Kit No. 60, 487 described and listed on the other side of this sheet. It provides all the additional materials needed for a thorough appreciation of Dr. Oster's theories. Price - \$8.00.

Equipment contained in the Accessory Kit is required for use in the following sections of the text:

<u>Section</u>	<u>Page</u>	<u>Equipment Included in Kit</u>
I	7	Front surface mirror (3" x 4" x 1/4" thick); one-way mirror (3" x 4" film)
III	10	Transmission and reflecting-type diffraction grating film (one sheet each, 2" x 4")
IV	12, 13	Ronchi gratings on film (2" x 3", 150 and 133 lines to the inch); front surface mirror; convex (enlarging), concave (diverging) and cylindrical lenses.
VII	20, 22	Convex (converging) lens; large, silver-colored balloon (approx. 12")
VIII	22, 23	One red and one blue 2" x 2", acetate-type filters; calcite crystal (approximately 3/4" x 1" x 1/2" thick.)
<hr/>		
<u>Appendix</u>		
B	26	One concave and one convex lens
E	30	Calcite crystal and a 2" x 2" sheet of polarizing film

Recommended for Group Use

If you have purchased Student's and Experimenter's Moiré Kit (Nos. 70, 718 or 60, 462) for use in the classroom, laboratory, etc., where it will receive heavy use, we suggest you send for the Educator's and Designer's Kit (Nos. 70, 719 or 60, 464) which have heavier, more durable pattern sheets. See full description on reverse side.

How to Exhaust All Pattern Potentials

An infinite variety of moiré patterns can be produced with the 8 transparencies and 8 opaque prints included in each Moiré Kit. However; many, many more possibilities are opened up when you combine, for example, two or more of the same transparencies and perhaps an opaque print. For this purpose we offer each kit without the text, at \$2.00 less. Such an additional set could add vastly to your experimental tools. See reverse side of this sheet.

Useful Accessories Sold Separately

For linear measurement of the intricacies of moiré patterns, order the Edscorp Pocket Comparator No. 30, 324....\$19.75 Ppd. Has 20mm-long reticle scale graduated in 200 parts, or every 0.1 mm. Complete with leather case. (See page 83 of Edmund Catalog 651.)

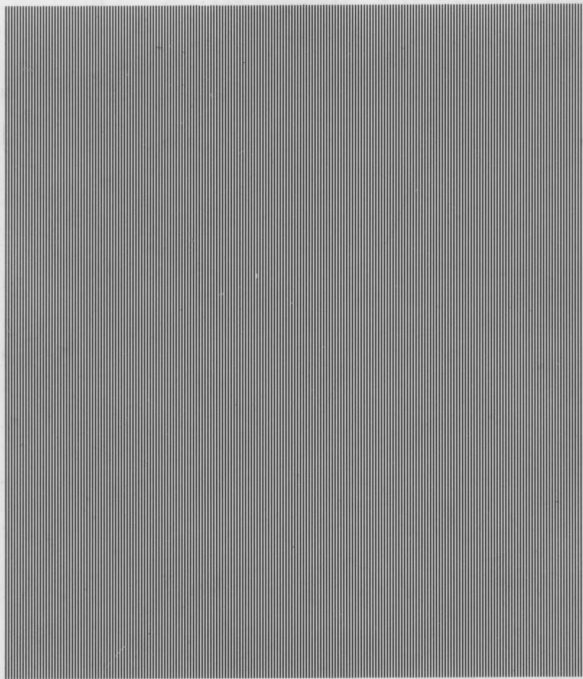
For moiré theory and graphic arts work, order the Edmund Halftone Screen Determiner. No. 40, 751 \$2.25 Ppd. (See reverse side of this sheet.)

EDMUND SCIENTIFIC CO. 101 East Gloucester Pike Barrington, N. J. 08007



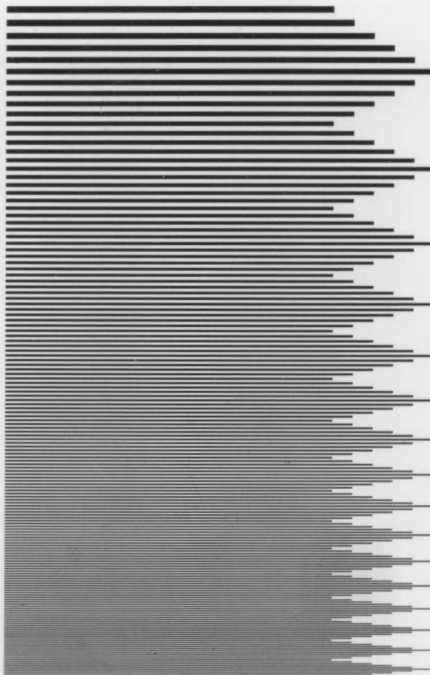
EDMUND SCIENTIFIC CO.
BARRINGTON, N. J.

MOIRE PATTERN NO. 1



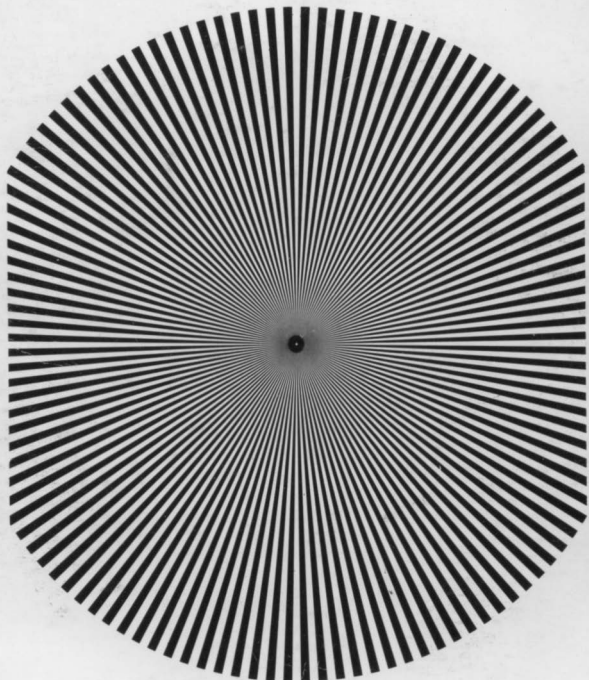
EDMUND SCIENTIFIC CO.
BARRINGTON, N. J.

MOIRE PATTERN NO. 2



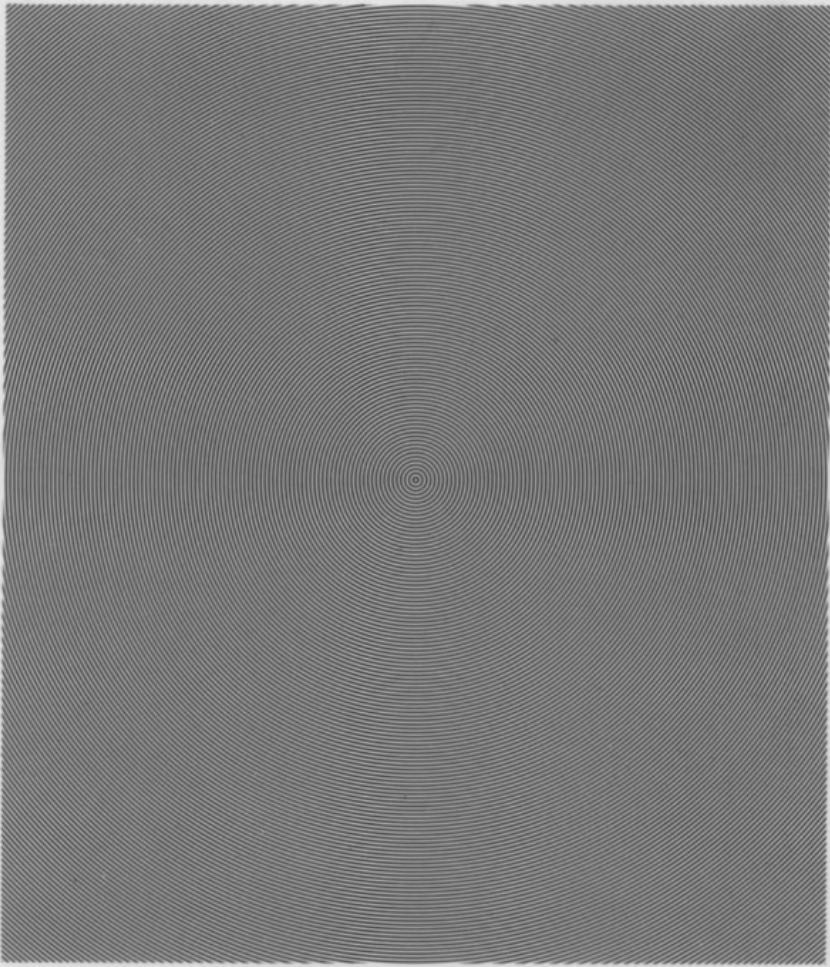
EDMUND SCIENTIFIC CO.
BARRINGTON, N. J.

MOIRE PATTERN NO. 3



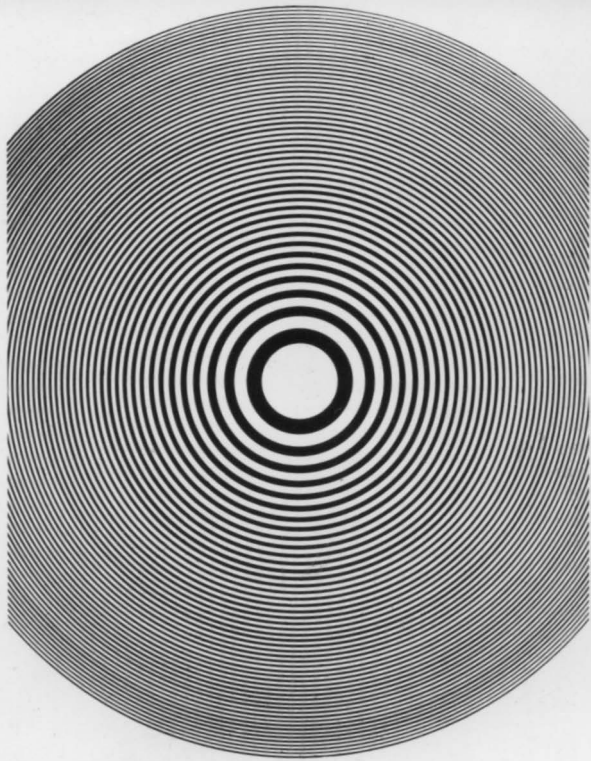
EDMUND SCIENTIFIC CO.
BARRINGTON, N. J.

MOIRE PATTERN NO. 4



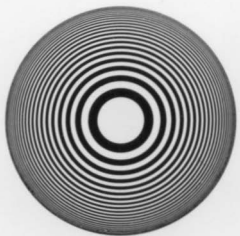
EDMUND SCIENTIFIC CO.
BARRINGTON, N. J.

MOIRE PATTERN NO. 5



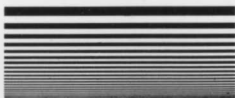
EDMUND SCIENTIFIC CO.
BARRINGTON, N. J.

MOIRE PATTERN NO. 6



EDMUND SCIENTIFIC CO.
BARRINGTON, N. J.

MOIRE PATTERN NO. 7



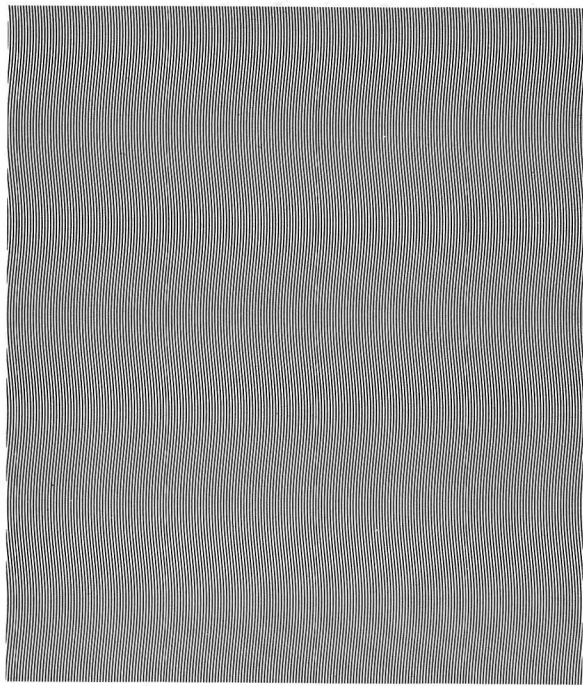
EDMUND SCIENTIFIC CO.
BARRINGTON, N. J.

MOIRE PATTERN NO. 8



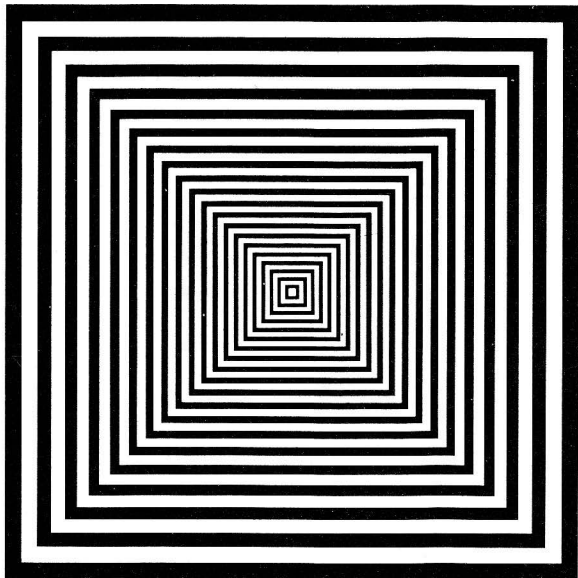
EDMUND SCIENTIFIC CO.
BARRINGTON, N. J.

MOIRE PATTERN NO. 11



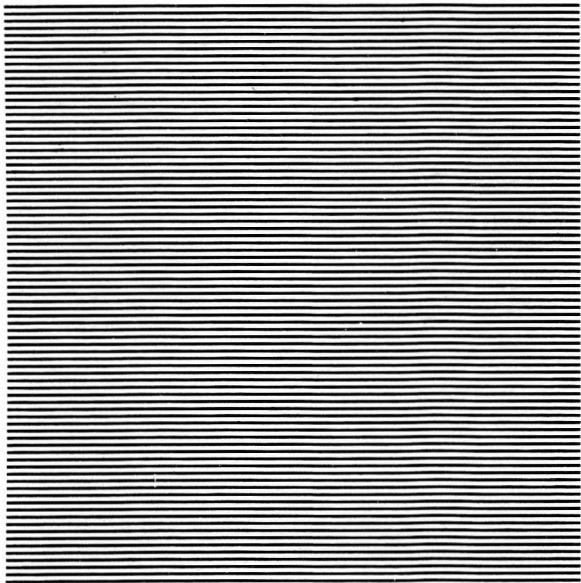
EDMUND SCIENTIFIC CO.
BARRINGTON, N. J.

MOIRE PATTERN NO. 12



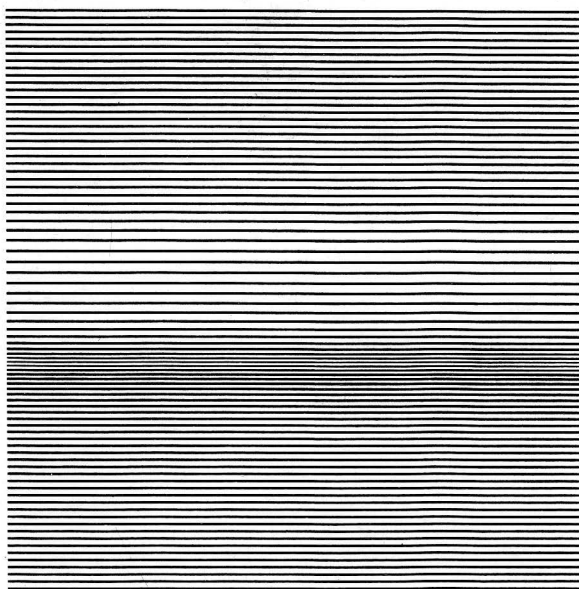
EDMUND SCIENTIFIC CO.
BARRINGTON, N. J.

MOIRE PATTERN NO. 13



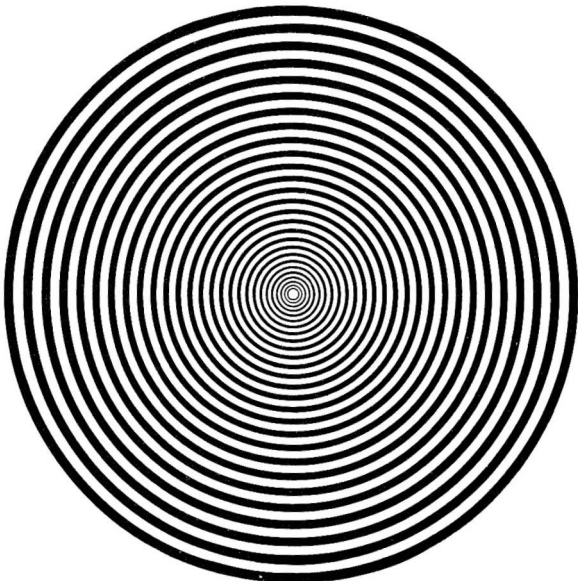
EDMUND SCIENTIFIC CO.
BARRINGTON, N. J.

MOIRE PATTERN NO. 14



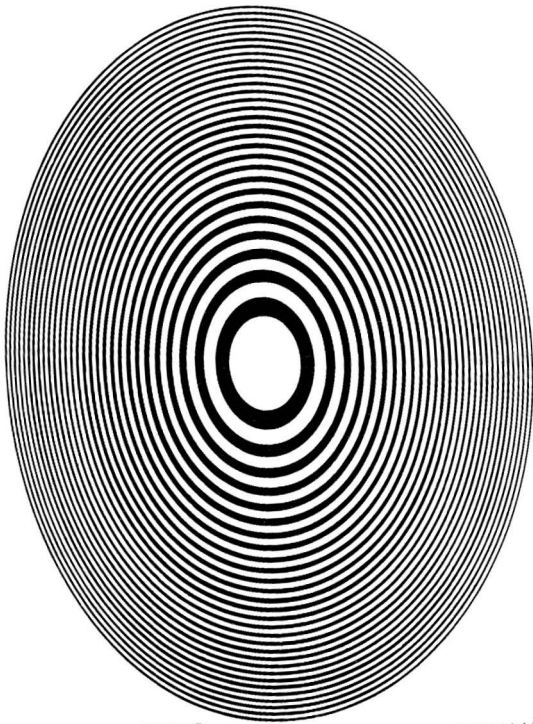
EDMUND SCIENTIFIC CO.
BARRINGTON, N. J.

MOIRE PATTERN NO. 15



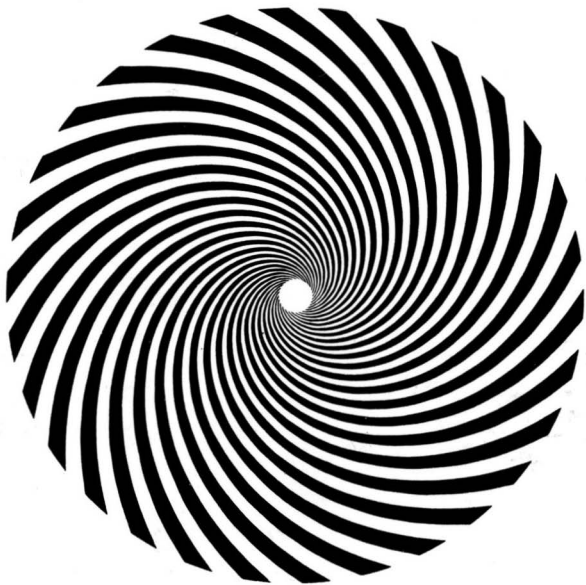
EDMUND SCIENTIFIC CO.
BARRINGTON, N. J.

MOIRE PATTERN NO. 16



EDMUND SCIENTIFIC CO.
BARRINGTON, N. J.

MOIRE PATTERN NO. 17



EDMUND SCIENTIFIC CO.
BARRINGTON, N. J.

MOIRE PATTERN NO. 18